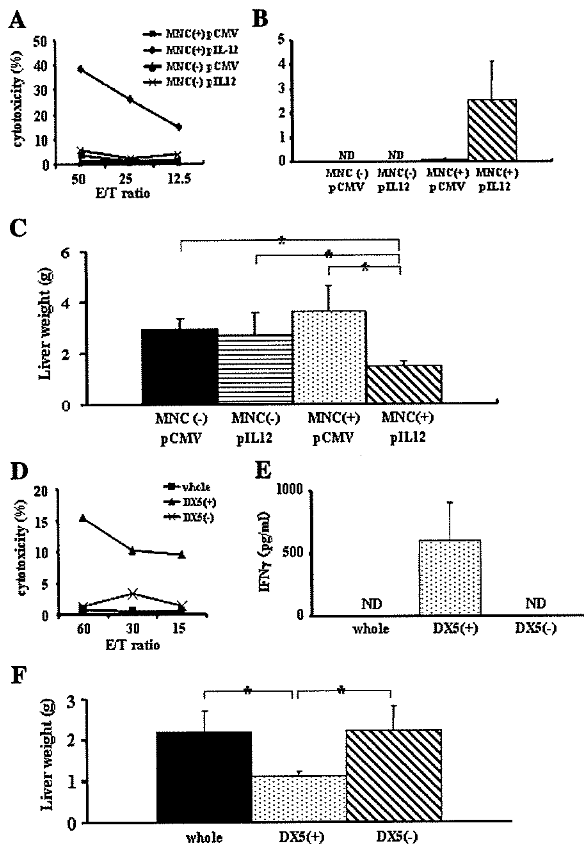

Fig. 5 Adoptive transfer of wild-type cells into GKO mice. Adoptive transfer of wild-type splenocytes restored anti-tumor effects of IL-12 in GKO mice. **a** GKO mice were intravenously injected with or without 2.0×10^8 splenocytes from wild-type mice and, 1 day later, hydrodynamically injected with either pCMV-IL-12 or pCMV. Mice were killed 4 days after plasmid injection. Yac1 lytic ability of hepatic mononuclear cells was expressed as the indicated effector and target ratios (E/T ratio). Experiments were done 3 times and representative data are shown. **b** and **c** GKO mice were intrasplenically injected with CT-26 cells and, 1 day later, intravenously injected with or without 2.0×10^8 splenocytes from wild-type mice. Two days after CT-26 injection, mice were hydrodynamically injected with either pCMV-IL-12 or pCMV. **b** The levels of serum IFNγ 4 days after plasmid injection are expressed as mean and SD ($n = 6$/group). **c** Fourteen days after plasmid injection, mice were killed to examine liver tumor development by measuring liver weight. The results are indicated as mean and SD ($n = 6$/group). *ND* not detectable. $^*p < 0.01$. Adoptive transfer of wild-type NK cells, but not non-NK cells, restored anti-tumor effects of IL-12 in GKO mice. **d** Wild-type splenocytes were purified into $DX5^+$ cells and $DX5^-$ cells. GKO mice were intravenously injected with 4.0×10^6 whole mononuclear cells or $DX5^+$ cells or $DX5^-$ cells and, 1 day later, hydrodynamically injected with either pCMV-IL-12 or pCMV. Mice were killed 4 days after hydrodynamic injection. Yac1 lytic ability of hepatic mononuclear cells is expressed as the indicated effector and target ratios (E/T ratio). Experiments were done 3 times and representative data are shown. **e** and **f** GKO mice were intrasplenically injected with CT-26 cells and, 1 day later, intravenously injected with whole mononuclear cells, $DX5^+$ cells or $DX5^-$ cells (4.0×10^6/mouse). Two days after CT-26 injection, mice were hydrodynamically injected with either pCMV-IL-12 or pCMV. **e** The levels of serum IFNγ are expressed as mean and SD ($n = 6$/group). **f** Fourteen days after plasmid injection, mice were killed to examine liver tumor development by measuring liver weight. The results are expressed as mean and SD ($n = 6$/group). *ND* not detectable. $^*p < 0.001$

serum levels of IP-10 and MIG, chemokines downstream of IFNγ, were measured after IL-12 therapy (Fig. 6e). pCMV-IL-12-injected mice showed significant increase in both levels compared with pCMV-injected mice. Significant increase after pCMV-IL-12 injection was also found in NK cell-depleted mice, but not in GKO mice. This result suggests that production of these chemokines was not completely suppressed in NK cell-depleted mice in our experimental condition. Immunohistochemical analysis revealed that tumoral accumulation of CD4-positive cells and CD8-positive cells was observed in pCMV-IL-12-injected mice but not in pCMV-injected mice. On the other hand, similar levels of CD31 expression were observed in tumors of pCMV-injected mice and pCMV-IL-12-injected mice (Fig. 6d). These results suggest that IL-12's anti-tumor effects might be mediated by T-cell accumulating in the tumor rather than anti-angiogenesis.

Discussion

IL-12 is recognized as a master regulator of adaptive type 1, cell-mediated immunity. One major action of IL-12 is its induction of other cytokines, particularly IFNγ. A large amount of evidence has indicated that IL-12 administration leads to IFNγ production from a variety of immune cells, such as T cells [16], B cells [17], NK cells [18] and NKT cells [22]. The relative impact of each immune cell as the source of IFNγ has been controversial. The present study highlighted NK cells as a most efficient producer of IFNγ that is critical for IL-12-induced anti-tumor effects.

Flow cytometric analysis revealed higher in vivo production of IFNγ of NK cells than that of other cell types. The levels of serum IFNγ were around fourfold higher in Rag2 KO mice which only possess NK cells than in wild-type mice. On the other hand, NK-cell depletion in wild-type mice led to twofold reduction of serum IFNγ levels. These data indicate substantial contribution of NK cells in IFNγ production in vivo. Previous research has demonstrated that the specific cellular effects of IL-12 are due mainly to activation of STAT4 [23, 24]. IL-12-induced STAT4 phosphorylation leads to the production of IFNγ [25]. In agreement with these reports, our in vitro analysis showed that, in contrast to STAT1, STAT4 was directly phosphorylated upon IL-12 stimulation, being independent of IFNγ. Of interest is the finding that NK cells express higher levels of STAT4 than non-NK cells, suggesting that NK cells possess an ideal expression profile of STATs for producing IFNγ upon IL-12 stimulation. Indeed, in vitro analysis revealed that NK cells, upon IL-12 exposure, displayed higher levels of IFNγ production as well as STAT4 phosphorylation than non-NK cells. These in vitro

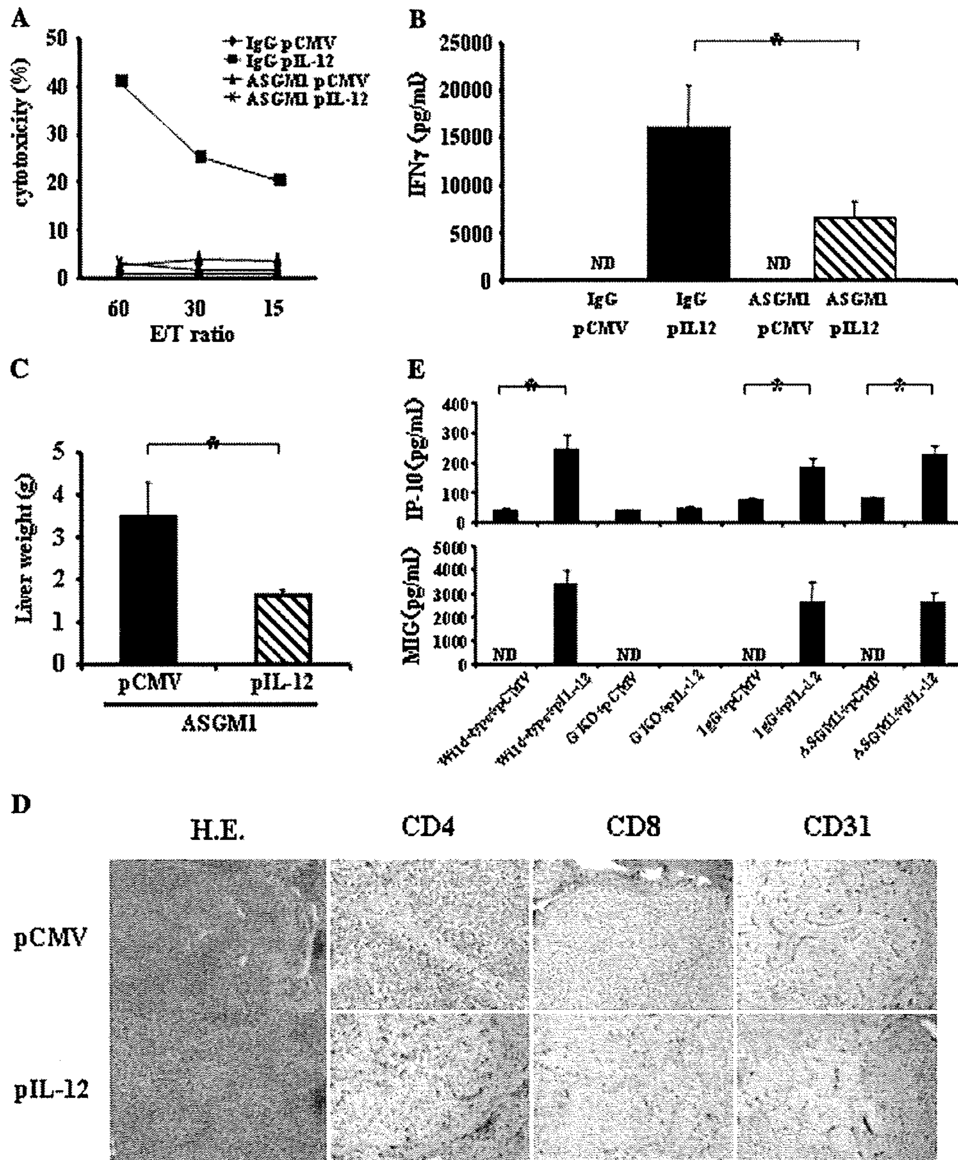

Fig. 6 Anti-tumor effects of IL-12 in NK-cell-depleted mice. Serum IFNγ levels and NK-cell activation. Wild-type mice were intraperitoneally injected with either anti-asialoGM1 antibody (ASGM1) or control IgG, and, 1 day later hydrodynamically injected with either pCMV-IL-12 or pCMV. Mice were killed 4 days after plasmid injection. **a** Yac1 lytic ability of hepatic mononuclear cells is expressed as the indicated effector and target ratios (E/T ratio). Experiments were done 2 times and representative data are shown. **b** The levels of serum IFNγ are expressed as mean and SD ($n = 6$/group). *ND* not detectable. $*p < 0.005$. Anti-metastatic effects. Wild-type mice were intrasplenically injected with CT-26 cells and, 1 day later and then every 5 days, intraperitoneally injected with either anti-asialoGM1 antibody (ASGM1) or control IgG, and hydrodynamically injected with either pCMV-IL-12 or pCMV 2 days after CT-26 injection. Fourteen days after plasmid injection, mice were killed to examine liver tumor development by measuring liver weight. **c** The results are indicated as mean and SD ($n = 6$/group). $*p < 0.001$. **d** Representative histology of liver sections analyzed by hematoxylin-eosin staining and immunohistochemistry of CD4, CD8 and CD31. **e** Serum levels of IP-10 and MIG. Wild-type or GKO mice were hydrodynamically injected with either pCMV-IL-12 or pCMV. Wild-type mice were intraperitoneally injected with either anti-asialoGM1 antibody (ASGM1) or control IgG, and 1 day later hydrodynamically injected with either pCMV-IL-12 or pCMV. Four days later, each mice were bled to measure the levels of serum IP-10 and MIG. Results are expressed as mean and SD ($n = 6$/group). *ND* not detectable. $*p < 0.001$

data are consistent with the in vivo observation that NK cells are efficient producers of IFNγ during IL-12 therapy.

Many studies have demonstrated that IFNγ production is required for the anti-tumor effects of IL-12 [14, 26, 27]. In fact, we have demonstrated that deletion of IFNγ abolished NK cytotoxicity and the anti-metastatic effect of IL-12 therapy in the liver. A large amount of evidence supports the concept that a major action of IL-12 is to promote the differentiation of naïve CD4 + T cells into Th1 cells, which produce IFNγ. Previous research reported that CD4

T-cell depletion caused inhibition of anti-tumor effects. More recent studies have supported a critical role of IFNγ as a third signal for CD8 T-cell differentiation. There have been many reports focusing on IFNγ production from T cells induced by IL-12 for the anti-tumor effect of IL-12 [28]. Segal et al. performed an elegant study showing a critical role of T-cell production of IFNγ in the anti-tumor effect by adoptively transferring T cells into GKO mice in a subcutaneous tumor model [29]. However, apart from this study, little is known about the contribution of each immune cell as a producer of IFNγ in terms of an anti-tumor effect. In our model, T-cell mediated adaptive responses were not required for the anti-metastatic effect of IL-12. More importantly, the anti-metastatic effects of IL-12 were restored in GKO mice by an adoptive transfer of wild-type NK cells. The same number of non-NK cells could not provoke IL-12-induced anti-tumor effects in GKO mice. The present study demonstrated for the first time a potent effect of NK cells on producing IFNγ that was critical for anti-metastatic effect during IL-12 therapy.

Our study showed that the main IFNγ producer of IL-12 was NK cells. So we focused on NK cells which were activated by IL-12 in an IFNγ-dependent manner to examine the cellular mechanism of protection against hepatic metastasis. Many studies have shown the importance of each subset (NK- [12], NKT- [10] and T [9, 30] cells) for anti-tumor effects of IL-12. In the present study, NK cells were sufficient while T cells, B cells, NKT cells were dispensable for IL-12-mediated NK-cell activation and anti-metastatic effects as IL-12 therapy showed Yac1 lytic ability and antimetastatic effects in Rag2 KO mice. On the other hand, NK-cell depletion by a repeated injection of anti-aialoGM1 antibody protected wild-type mice from macroscopic liver metastasis, but did not from microscopic liver metastasis. Thus, although NK cells were required for a full-blown IL-12 anti-tumor effect, other anti-tumor pathways are activated by IL-12 in the absence of NK cells. Serum levels of IP-10 and MIG suggest that production of these chemokines downstream of IFNγ was not suppressed in NK-cell-depleted mice in our experimental condition. When compared with the experiment on GKO mice, accumulation of CD4-positive cells and CD8-positive cells were more evident in NK-cell-depleted mice than in GKO mice (Supplementary Figure). On the other hand, there was no remarkable difference in the expression of CD31 between pCMV injection and pCMV-IL-12 injection. These results suggested that in NK-cell-depleted mice IL-12 may exert anti-tumor effect via T-cell accumulation rather than anti-angiogenesis.

Since the liver contains an abundance of immune cells (especially NK cells) [31], the cytokine-mediated activation of these cells may be a promising approach toward anti-tumor therapy in this organ [32]. IL-12 is a cytokine known to elicit a potent anti-tumor effect in mouse experimental models. However, clinical trials attempted to date were interrupted by fatal adverse effects. Systemic IL-12 therapy has been associated with dose-limiting toxicity [33]. IL-12 induces activation of the pro-inflammatory pathway which causes the complications of high dose cytokine, independent of the action of IFNγ [34]. On the other hand, the levels of immunosuppressive cytokine, for example, TGF-β1 or IL-10 were significantly higher in patients with hepatocellular cancer and colon cancer [35–38]. In particular, TGF-β1 in serum can limit NK-cell IFNγ production [39]. Thus, in patients with advanced disease, IL-12 may not be able to exert its potent anti-tumor immune-effects because IFNγ, which is an important mediator of the IL-12-induced immune response, is less effective in a tumor environment. In the present study, we demonstrated that NK-cell IFNγ production induced by IL-12 was sufficient for the anti-metastatic effect of IL-12 in the liver. Thus, a strategy of efficiently producing IFNγ from NK cells may be important for avoiding toxicity of IL-12 therapy.

IL-12 gene therapy has an advantage to allow local production of the cytokine at the tumor sites with low serum concentration. Studies demonstrated that intratumoral administration of adenovirus encoding IL-12 to animals with different types of carcinoma caused complete tumor eradication and increased long-term survival [40, 41]. Moreover, injection of IL-12-encoding adenovirus in one nodule of liver tumor resulted in regression of distant nodules in the liver [41]. However, in a clinical trial anti-tumor activity of IL-12-encoding adenovirus was only observed in the injected tumor sites, but not in distant tumors [42]. The present study shed light on hydrodynamic transfection of hepatocytes as a promising strategy to eradicate disseminated tumors from whole liver.

In summary, NK cells are not just an effector for innate immunity but a mediator producing IFNγ that is critical for the IL-12 anti-tumor effects. Extremely higher expression of STAT4 may be a basis for efficient production of IFNγ from NK cells.

Acknowledgments We thank Dr. Morihiro Watanabe (Laboratory of Experimental Immunology, Division of Basic Sciences, National Cancer Institute-Frederick Cancer Research and Development Center) for providing the pCMV-IL-12 plasmid, Dr. Yoichiro Iwakura (University of Tokyo, Institute of Medical Science) for providing GKO mice.

References

1. Kobayashi M, Fitz L, Ryan M, Hewick RM, Clark SC, Chan S, Loudon R, Sherman F, Perussia B, Trinchieri G (1989) Identification and purification of natural killer cell stimulatory factor

(NKSF), a cytokine with multiple biologic effects on human lymphocytes. J Exp Med 170(3):827–845
2. Stern AS, Podlaski FJ, Hulmes JD, Pan YC, Quinn PM, Wolitzky AG, Familletti PC, Stremlo DL, Truitt T, Chizzonite R, Gately MK (1990) Purification to homogeneity and partial characterization of cytotoxic lymphocyte maturation factor from human B-lymphoblastoid cells. Proc Natl Acad Sci USA 87(17):6808–6812
3. Watford WT, Moriguchi M, Morinobu A, O'Shea JJ (2003) The biology of IL-12: coordinating innate and adaptive immune responses. Cytokine Growth Factor Rev 14(5):361–368
4. Trinchieri G (2003) Interleukin-12 and the regulation of innate resistance and adaptive immunity. Nat Rev Immunol 3(2):133–146
5. Colombo MP, Trinchieri G (2002) Interleukin-12 in anti-tumor immunity and immunotherapy. Cytokine Growth Factor Rev 13(2):155–168
6. Del Vecchio M, Bajetta E, Canova S, Lotze MT, Wesa A, Parmiani G, Anichini A (2007) Interleukin-12: biological properties and clinical application. Clin Cancer Res 13(16):4677–4685
7. Wigginton JM, Gruys E, Geiselhart L, Subleski J, Komschlies KL, Park JW, Wiltrout TA, Nagashima K, Back TC, Wiltrout RH (2001) IFN-gamma and Fas/FasL are required for the antitumor and antiangiogenic effects of IL-12/pulse IL-2 therapy. J Clin Invest 108(1):51–62
8. Lee JC, Kim DC, Gee MS, Saunders HM, Sehgal CM, Feldman MD, Ross SR, Lee WM (2002) Interleukin-12 inhibits angiogenesis and growth of transplanted but not in situ mouse mammary tumor virus-induced mammary carcinomas. Cancer Res 62(3):747–755
9. Brunda MJ, Luistro L, Warrier RR, Wright RB, Hubbard BR, Murphy M, Wolf SF, Gately MK (1993) Antitumor and antimetastatic activity of interleukin 12 against murine tumors. J Exp Med 178(4):1223–1230
10. Cui J, Shin T, Kawano T, Sato H, Kondo E, Toura I, Kaneko Y, Koseki H, Kanno M, Taniguchi M (1997) Requirement for Valpha14 NKT cells in IL-12-mediated rejection of tumors. Science 278(5343):1623–1626
11. Zilocchi C, Stoppacciaro A, Chiodoni C, Parenza M, Terrazzini N, Colombo MP (1998) Interferon gamma-independent rejection of interleukin 12-transduced carcinoma cells requires CD4 + T cells and Granulocyte/Macrophage colony-stimulating factor. J Exp Med 188(1):133–143
12. Kodama T, Takeda K, Shimozato O, Hayakawa Y, Atsuta M, Kobayashi K, Ito M, Yagita H, Okumura K (1999) Perforin-dependent NK cell cytotoxicity is sufficient for anti-metastatic effect of IL-12. Eur J Immunol 29(4):1390–1396
13. Takeda K, Hayakawa Y, Atsuta M, Hong S, Van Kaer L, Kobayashi K, Ito M, Yagita H, Okumura K (2000) Relative contribution of NK and NKT cells to the anti-metastatic activities of IL-12. Int Immunol 12(6):909–914
14. Ogawa M, Yu WG, Umehara K, Iwasaki M, Wijesuriya R, Tsujimura T, Kubo T, Fujiwara H, Hamaoka T (1998) Multiple roles of interferon-gamma in the mediation of interleukin 12-induced tumor regression. Cancer Res 58(11):2426–2432
15. Subleski JJ, Hall VL, Back TC, Ortaldo JR, Wiltrout RH (2006) Enhanced antitumor response by divergent modulation of natural killer and natural killer T cells in the liver. Cancer Res 66(22):11005–11012
16. Kubin M, Kamoun M, Trinchieri G (1994) Interleukin 12 synergizes with B7/CD28 interaction in inducing efficient proliferation and cytokine production of human T cells. J Exp Med 180(1):211–222
17. Yoshimoto T, Okamura H, Tagawa YI, Iwakura Y, Nakanishi K (1997) Interleukin 18 together with interleukin 12 inhibits IgE production by induction of interferon-gamma production from activated B cells. Proc Natl Acad Sci USA 94(8):3948–3953
18. Lauwerys BR, Renauld JC, Houssiau FA (1999) Synergistic proliferation and activation of natural killer cells by interleukin 12 and interleukin 18. Cytokine 11(11):822–830
19. Takehara T, Uemura A, Tatsumi T, Suzuki T, Kimura R, Shiotani A, Ohkawa K, Kanto T, Hiramatsu N, Hayashi N (2007) Natural killer cell-mediated ablation of metastatic liver tumors by hydrodynamic injection of IFNalpha gene to mice. Int J Cancer 120(6):1252–1260
20. Watanabe M, Fenton RG, Wigginton JM, McCormick KL, Volker KM, Fogler WE, Roessler PG, Wiltrout RH (1999) Intradermal delivery of IL-12 naked DNA induces systemic NK cell activation and Th1 response in vivo that is independent of endogenous IL-12 production. J Immunol 163(4):1943–1950
21. Takehara T, Suzuki T, Ohkawa K, Hosui A, Jinushi M, Miyagi T, Tatsumi T, Kanazawa Y, Hayashi N (2006) Viral covalently closed circular DNA in a non-transgenic mouse model for chronic hepatitis B virus replication. J Hepatol 44(2):267–274
22. Shin T, Nakayama T, Akutsu Y, Motohashi S, Shibata Y, Harada M, Kamada N, Shimizu C, Shimizu E, Saito T, Ochiai T, Taniguchi M (2001) Inhibition of tumor metastasis by adoptive transfer of IL-12-activated Valpha14 NKT cells. Int J Cancer 91(4):523–528
23. Thierfelder WE, van Deursen JM, Yamamoto K, Tripp RA, Sarawar SR, Carson RT, Sangster MY, Vignali DA, Doherty PC, Grosveld GC, Ihle JN (1996) Requirement for Stat4 in interleukin-12-mediated responses of natural killer and T cells. Nature 382(6587):171–174
24. Kaplan MH, Sun YL, Hoey T, Grusby MJ (1996) Impaired IL-12 responses and enhanced development of Th2 cells in Stat4-deficient mice. Nature 382(6587):174–177
25. Morinobu A, Gadina M, Strober W, Visconti R, Fornace A, Montagna C, Feldman GM, Nishikomori R, O'Shea JJ (2002) STAT4 serine phosphorylation is critical for IL-12-induced IFN-gamma production but not for cell proliferation. Proc Natl Acad Sci USA 99(19):12281–12286
26. Comes A, Di Carlo E, Musiani P, Rosso O, Meazza R, Chiodoni C, Colombo MP, Ferrini S (2002) IFN-gamma-independent synergistic effects of IL-12 and IL-15 induce anti-tumor immune responses in syngeneic mice. Eur J Immunol 32(7):1914–1923
27. Hafner M, Falk W, Echtenacher B, Mannel DN (1999) Interleukin-12 activates NK cells for IFN-gamma-dependent and NKT cells for IFN-gamma-independent antimetastatic activity. Eur Cytokine Netw 10(4):541–548
28. Komita H, Homma S, Saotome H, Zeniya M, Ohno T, Toda G (2006) Interferon-gamma produced by interleukin-12-activated tumor infiltrating CD8 + T cells directly induces apoptosis of mouse hepatocellular carcinoma. J Hepatol 45(5):662–672
29. Segal JG, Lee NC, Tsung YL, Norton JA, Tsung K (2002) The role of IFN-gamma in rejection of established tumors by IL-12: source of production and target. Cancer Res 62(16):4696–4703
30. Nastala CL, Edington HD, McKinney TG, Tahara H, Nalesnik MA, Brunda MJ, Gately MK, Wolf SF, Schreiber RD, Storkus WJ, Lotze MT (1994) Recombinant IL-12 administration induces tumor regression in association with IFN-gamma production. J Immunol 153(4):1697–1706
31. Doherty DG, O'Farrelly C (2000) Innate and adaptive lymphoid cells in the human liver. Immunol Rev 174:5–20
32. Seki S, Habu Y, Kawamura T, Takeda K, Dobashi H, Ohkawa T, Hiraide H (2000) The liver as a crucial organ in the first line of host defense: the roles of Kupffer cells, natural killer (NK) cells and NK1.1 Ag + T cells in T helper 1 immune responses. Immunol Rev 174:35–46
33. Car BD, Eng VM, Lipman JM, Anderson TD (1999) The toxicology of interleukin-12: a review. Toxicol Pathol 27(1):58–63
34. Biber JL, Jabbour S, Parihar R, Dierksheide J, Hu Y, Baumann H, Bouchard P, Caligiuri MA, Carson W (2002) Administration of

two macrophage-derived interferon-gamma-inducing factors (IL-12 and IL-15) induces a lethal systemic inflammatory response in mice that is dependent on natural killer cells but does not require interferon-gamma. Cell Immunol 216(1–2):31–42

35. Tsushima H, Ito N, Tamura S, Matsuda Y, Inada M, Yabuuchi I, Imai Y, Nagashima R, Misawa H, Takeda H, Matsuzawa Y, Kawata S (2001) Circulating transforming growth factor beta 1 as a predictor of liver metastasis after resection in colorectal cancer. Clin Cancer Res 7(5):1258–1262
36. Okumoto K, Hattori E, Tamura K, Kiso S, Watanabe H, Saito K, Saito T, Togashi H, Kawata S (2004) Possible contribution of circulating transforming growth factor-beta1 to immunity and prognosis in unresectable hepatocellular carcinoma. Liver Int 24(1):21–28
37. Chau GY, Wu CW, Lui WY, Chang TJ, Kao HL, Wu LH, King KL, Loong CC, Hsia CY, Chi CW (2000) Serum interleukin-10 but not interleukin-6 is related to clinical outcome in patients with resectable hepatocellular carcinoma. Ann Surg 231(4):552–558
38. Galizia G, Lieto E, De Vita F, Romano C, Orditura M, Castellano P, Imperatore V, Infusino S, Catalano G, Pignatelli C (2002) Circulating levels of interleukin-10 and interleukin-6 in gastric and colon cancer patients before and after surgery: relationship with radicality and outcome. J Interferon Cytokine Res 22(4):473–482
39. Meadows SK, Eriksson M, Barber A, Sentman CL (2006) Human NK cell IFN-gamma production is regulated by endogenous TGF-beta. Int Immunopharmacol 6(6):1020–1028
40. Caruso M, Pham-Nguyen K, Kwong YL, Xu B, Kosai KI, Finegold M, Woo SL, Chen SH (1996) Adenovirus-mediated interleukin-12 gene therapy for metastatic colon carcinoma. Proc Natl Acad Sci USA 93(21):11302–11306
41. Barajas M, Mazzolini G, Genove G, Bilbao R, Narvaiza I, Schmitz V, Sangro B, Melero I, Qian C, Prieto J (2001) Gene therapy of orthotopic hepatocellular carcinoma in rats using adenovirus coding for interleukin 12. Hepatology 33(1):52–61
42. Sangro B, Mazzolini G, Ruiz J, Herraiz M, Quiroga J, Herrero I, Benito A, Larrache J, Pueyo J, Subtil JC, Olague C, Sola J et al (2004) Phase I trial of intratumoral injection of an adenovirus encoding interleukin-12 for advanced digestive tumors. J Clin Oncol 22(8):1389–1397

Anticancer Chemotherapy Inhibits MHC Class I–Related Chain A Ectodomain Shedding by Downregulating ADAM10 Expression in Hepatocellular Carcinoma

Keisuke Kohga, Tetsuo Takehara, Tomohide Tatsumi, Takuya Miyagi, Hisashi Ishida, Kazuyoshi Ohkawa, Tatsuya Kanto, Naoki Hiramatsu, and Norio Hayashi

Department of Gastroenterology and Hepatology, Osaka University Graduate School of Medicine, Osaka, Japan

Abstract

MHC class I–related chain A (MICA) is a ligand for the NKG2D-activating immunoreceptor that mediates activation of natural killer (NK) cells. The ectodomain of MICA is shed from tumor cells, which may be an important means of evading antitumor immunity. We previously reported that patients with hepatocellular carcinoma (HCC) display high levels of soluble MICA in circulation, which could be downregulated by chemotherapy. The present study shows that anti-HCC drugs suppress MICA ectodomain shedding by inhibiting expression of a disintegrin and metalloproteinase 10 (ADAM10). Both ADAM10 and CD44, a typical substrate of the ADAM10 protease, were expressed in human HCC tissues and HCC cells but not in normal liver tissues or cultured hepatocytes. Small interfering RNA–mediated knockdown experiments revealed that ADAM10 is a critical sheddase for both MICA and CD44 in HCC cells. Of interest is the finding that epirubicin clearly downregulated ADAM10 expression and MICA shedding in HCC cells; its suppressive effect on MICA shedding was abolished in ADAM10-depleted cells. Epirubicin treatment also enhanced the NKG2D-mediated NK sensitivity of HCC cells. Patients with HCC had significantly higher levels of serum-soluble CD44, which correlated well with serum-soluble MICA levels, thus suggesting a close link between ADAM10 activity and MICA shedding in these patients. Soluble MICA and CD44 levels were downregulated with a significant correlation in patients treated by transarterial chemoembolization using epirubicin. In conclusion, anticancer drugs can modulate expression of ADAM10, which is critically involved in MICA ectodomain shedding. Epirubicin therapy may have a previously unrecognized effect on antitumor immunity in HCC patients. [Cancer Res 2009;69(20):8050–7]

Introduction

Hepatocellular carcinoma (HCC) is one of the leading causes of cancer deaths worldwide. Chronic liver disease caused by hepatitis virus infection and nonalcoholic steatohepatitis leads to a predisposition for HCC, with liver cirrhosis, in particular, being considered a premalignant condition (1, 2). With regard to treatment, surgical resection or percutaneous techniques such as ethanol injection and radiofrequency ablation are considered to be choices for curable treatment of localized HCC, whereas transcatheter arterial chemoembolization (TACE) is a well-established technique for more advanced HCC (3). The liver contains a large compartment of innate immune cells [natural killer (NK) cells and natural killer T cells] and acquired immune cells (T cells; refs. 4, 5), but the activation of these immune cells after HCC treatments remains unclear. If such treatments can efficiently activate abundant immune cells in the liver, this could lead to the establishment of attractive new strategies for HCC treatment.

MHC class I–related chain A and B (MICA and MICB) are ligands for NKG2D expressed on a variety of immune cells (6). In contrast to classic MHC class I molecules, MICA/B are rarely expressed on normal cells but frequently on tumor cells (7–10). The engagement of MICA/B and NKG2D strongly activates NK cells and costimulates T cells, enhancing their cytolytic activity and cytokine production (11). Thus, the MICA/B-NKG2D pathway is an important mechanism by which the host immune system recognizes and kills transformed cells (12). In addition to those membrane-bound forms, MICA/B molecules are also cleaved proteolytically from tumor cells and appear as soluble forms in sera of patients with malignancy (13–15). Soluble MICA/B in circulation downregulates NKG2D expression and disturbs NKG2D-mediated antitumor immunity (9, 10, 13). We previously reported that soluble MICA could be detected in sera of HCC patients (16) and that TACE treatment reduces the levels of soluble MICA and thereby upregulates the expression of NKG2D (17). Thus, cancer therapy may have a beneficial effect on NKG2D-mediated immune responses.

The release of soluble MICA/B from tumor cells is impaired by metalloproteinase inhibitors, suggesting the involvement of members of the metzincin superfamily, such as ADAM proteins (14, 18). In addition, ERp5, related to protein disulfide isomerase, is required for the MICA shedding as it reduces disulfide bond of the α3 domain of MICA (19). Although it may not be a direct protease for MICA, it may enable proteolytic cleavage through conformational change. Recently, it was reported that MICA shedding of 293T fibroblast cells and HeLa cervical cancer cells was inhibited by silencing of the ADAM10 and ADAM17 proteases (20). This suggests that ADAM family proteins may be a therapeutic target for enhancing antitumor immunity, but how to therapeutically modulate these proteins is still not clear. Furthermore, it remains to be determined whether ADAMs can regulate MICA shedding in a clinical setting.

In the present study, we showed that ADAM10, but not ADAM17, was critically required for MICA shedding in human HCC cells. Of importance is the discovery that epirubicin, a widely used anti-HCC drug, was capable of downregulating ADAM10 expression and

Note: Supplementary data for this article are available at Cancer Research Online (http://cancerres.aacrjournals.org/).

K. Kohga, T. Takehara, and T. Tatsumi contributed equally to this work.

Requests for reprints: Norio Hayashi, Department of Gastroenterology and Hepatology, Osaka University Graduate School of Medicine, 2-2 Yamadaoka, Suita, Osaka 565-0871, Japan. Phone: 81-6-6879-3621; Fax: 81-6-6879-3629; E-mail: hayashin@gh.med.osaka-u.ac.jp.

©2009 American Association for Cancer Research.

doi:10.1158/0008-5472.CAN-09-0789

activity in HCC cells; it can thus inhibit MICA shedding and enhance NK sensitivity. ADAM10 was immunohistochemically detected in HCC tissues and a correlation was observed between soluble MICA levels and ADAM10 activity determined by soluble CD44 levels in HCC patients. The present study sheds light on previously unrecognized effects of an anticancer drug on modulating ADAM family proteins and MICA shedding and thus suggests a promising aspect for chemoimmunotherapy against human HCC.

Materials and Methods

Liver tissues and immunohistochemistry. Human HCC tissues (n = 8) and normal liver tissues (n = 2) obtained at surgical resection were used. Informed consent, under an institutional review board–approved protocol,

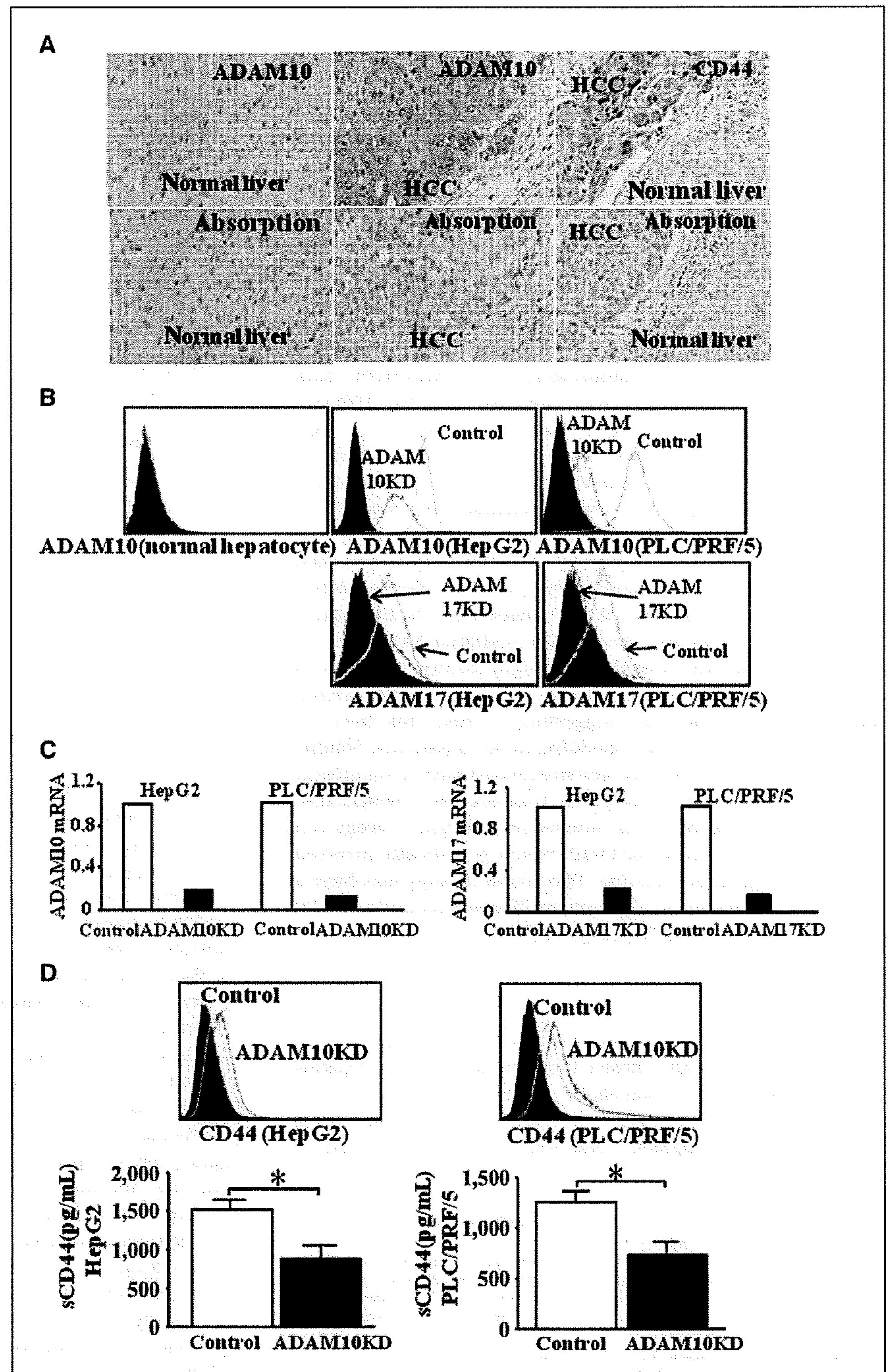

Figure 1. Expression of ADAM10 and CD44 in human HCC tissues and ADAM10 or ADAM17 knockdown in human HCC cells. *A,* immunohistochemical detection of ADAM10 and CD44 in human HCC tissues (n = 8) and normal liver tissues (n = 2). Liver sections were stained with the corresponding antibodies (*top panels*). Both primary antibodies were incubated with recombinant CD44 and ADAM10 proteins and then applied to liver sections in parallel as the absorption test (*bottom panels*). Representative images are shown. *B* and *C,* expression of ADAM10 or ADAM17 in human primary hepatocyte and HCC cell lines (*HepG2* and *PLC/PRF/5*). Cells were treated with ADAM10 siRNA, ADAM17 siRNA, or control siRNA, and subjected to analysis of ADAM10 or ADAM17 expression by flow cytometry (*B*) or real-time RT-PCR (*C*). *Histograms,* anti-ADAM10 or anti-ADAM17 staining of ADAM10 or ADAM17 siRNA-treated cells (*ADAM10KD* or *ADAM17KD, black dotted line*) and control siRNA-treated cells (*Control, gray line*), respectively. *Closed histograms,* control IgG staining. *D,* the expression of membrane-bound CD44 on HCC cells treated with ADAM10 siRNA (ADAM10KD, *black line*) or control siRNA (*Control, gray line*) was evaluated by flow cytometry (*top panels*). *Closed histograms,* control IgG staining. Soluble CD44 (*sCD44*) production from HCC cells treated with ADAM10 siRNA or control siRNA were evaluated by specific ELISA (*bottom panels*). *, $P < 0.05$.

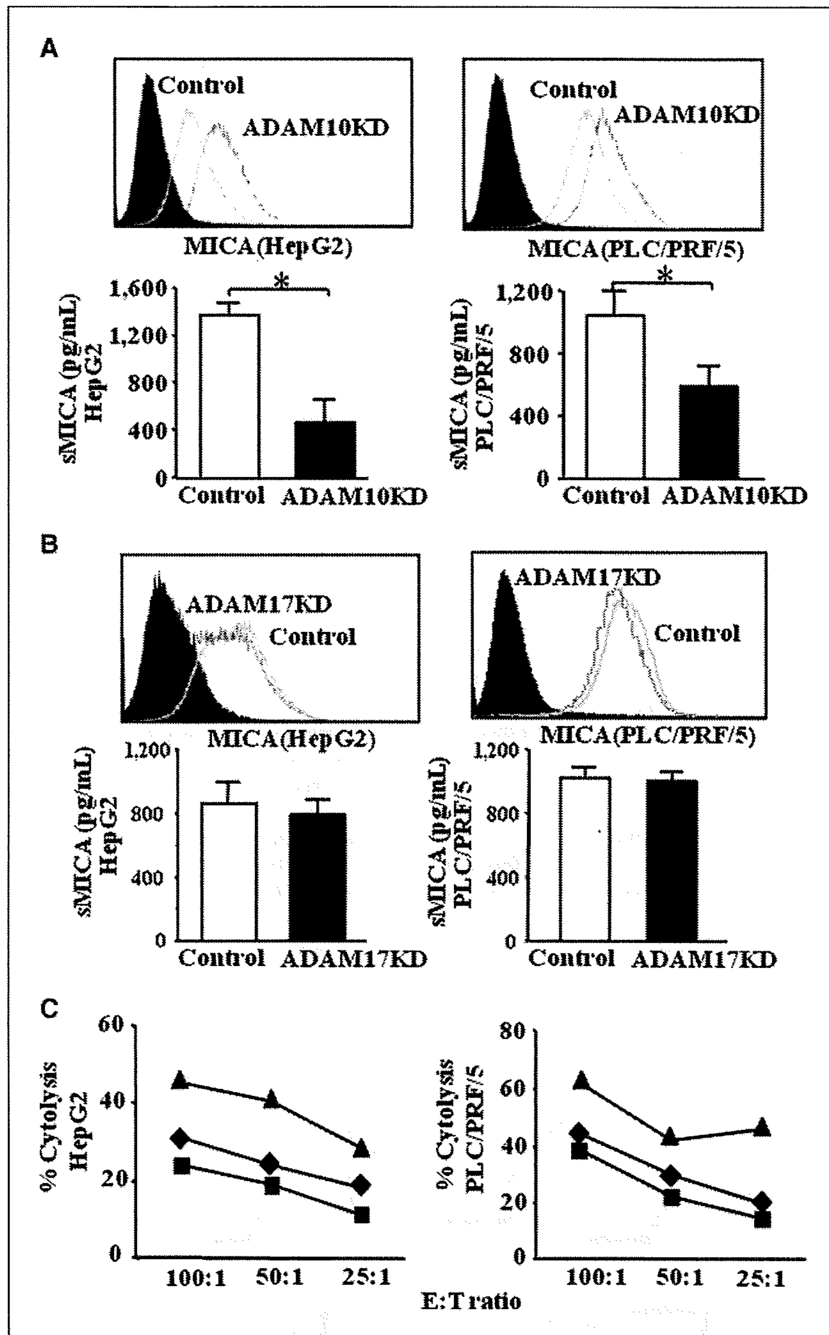

Figure 2. Expression of MICA in ADAM10 or ADAM17 knockdown HCC cells and NK sensitivity in ADAM10 knockdown HCC cells. *A* and *B*, the expression of membrane-bound MICA on HCC cells treated with ADAM10 siRNA (*ADAM10KD, black line*; *A*), ADAM17 siRNA (*ADAM17KD, black line*; *B*), or control siRNA (*Control, gray line*) was evaluated by flow cytometry (*top panels*). *Closed histograms,* control IgG staining. Soluble MICA (*sMICA*) production from HCC cells treated with ADAM10 siRNA (*A*), ADAM17 siRNA (*B*), or control siRNA were evaluated by specific ELISA (*bottom panels*). *, $P < 0.05$. *C*, HCC cells treated with ADAM10 siRNA or control siRNA were subjected to ^{51}Cr-release assay against NK cells. Cytolytic activity of NK cells against control HCC cells (■) or ADAM10 knockdown HCC cells without (▲) or with blocking antibody of MICA/B (6D4; ♦). Representative results are shown. Similar results were obtained from three independent experiments.

was obtained from all patients before sample acquisition. Liver sections were subjected to immunohistochemical staining using the ABC procedure (Vector Laboratories, Burlingame, CA). The primary antibodies used were anti-ADAM10 and anti-CD44 (R&D Systems). To confirm the specificity of the staining, primary antibodies were incubated with recombinant CD44 or ADAM10 protein (R&D Systems, Minneapolis, MN) for 3 h and then applied onto liver sections in parallel with staining of the primary antibodies as the absorption test.

HCC cell lines. Human HCC cell lines HepG2 and PLC/PRF/5 were purchased from the American Type Culture Collection and were cultured with DMEM supplemented with 10% fetal bovine serum (GIBCO/Life Technologies, Grand Island, NY) in a humidified incubator at 5% CO_2 and 37°C.

RNA silencing. The small interfering RNA (siRNA) method was used to knockdown ADAM10 and ADAM17. Stealth RNAi oligonucleotide targeting ADAM10 or ADAM17 and scrambled oligonucleotides as a control were purchased from Invitrogen (Carlsbad, CA). Cells were transfected by RNAi Max transfection reagent (Invitrogen) with 50 nmol/L siRNA. At 24 h posttransfection, the cells were analyzed for specific depletion of the mRNAs of ADAM10 and ADAM17 by real-time reverse transcription-PCR (RT-PCR; Applied Biosystems, Foster City, CA). The following siRNAs were used: ADAM10, 5′-AUAUCUGGGCAAUCACAG-CUUCUCG-3′; scramble control, 5′-AUACUUGGUCAACGCACUUCGAUGG-3′; ADAM17, 5′-UGAACAAGCUCUUCAGGUGGUUCUC-3′; scramble control, 5′-UGAUUAGAACUCUCGACUGGUGCUC-3′.

ELISA. The supernatants of cultured cells were harvested at 24 h after transfection with siRNA as well as sera from HCC patients (n = 97) and age-matched healthy volunteers (n = 32) were subjected to analysis of soluble MICA and soluble CD44 levels. Informed consent, under an institutional review board–approved protocol, was obtained from all patients before sample acquisition. The levels of soluble MICA and soluble CD44 were

determined by DuoSet MICA eELISA kit (R&D Systems) and soluble CD44std ELISA (Abcam, Cambridge, MA), respectively.

Flow cytometry. For the detection of membrane-bound MICA and CD44, cells were incubated with an anti-MICA–specific antibody (2C10, Santa Cruz Biotechnology, Santa Cruz, CA) or anti-CD44 antibody (R&D Systems) and stained with phycoerythrin (PE)-goat anti-mouse immunoglobulin (Beckman Coulter) as a secondary reagent and then subjected to flow cytometric analysis. For the detection of ADAM10 or ADAM17, cells were fixed and permeabilized with Cytofix/Cytoperm (BD Biosciences, San Jose, CA) and stained with PE-conjugated anti-ADAM10 or anti-ADAM17 antibody (R&D Systems). Flow cytometric analysis was performed using a FACScan flow cytometer (Becton Dickinson).

Plasmid construction of pMyc-MICA. MICA full coding cDNA was isolated from Huh7, human HCC cells, using a conventional RT-PCR method (Supplementary Fig. S1, DDBJ/EMBL/Genbank accession number AB506764) and inserted into the *Hin*dIII-*Xba*I site of pcDNA3 (Invitrogen). A C-myc tag was placed between the leader peptide and the α1 domain of MICA by site-specific mutagenesis using a QuikChange site-directed mutagenesis kit (Stratagene, La Jolla, CA) referred to as pMyc-MICA. Cells were transfected with pMyc-MICA using a Lipofectamine LTX reagent (Invitrogen). The green fluorescent protein (GFP)–expressing vector (pEGFP-C1, Clontech, Mountain View, CA) was cotransfected to evaluate the transfection efficiency.

Immunoprecipitation. Cells or tissues were homogenized in lysis buffer containing 1% NP40, 0.5% sodium deoxycholate, 0.1% SDS, 50 μg/mL aprotinin, 100 μg/mL phenylmethylsulfonyl fluoride, 1 mmol/L sodium orthovanadate, 50 mmol/L sodium fluoride, and PBS. To the cell supernatants, 0.5% NP40 and a cocktail of protease inhibitors were added. The protein contents of the samples were determined by BCA protein assay kit (Pierce, Rackford, IL). Immunoprecipitation with anti–c-Myc beads was performed for 1 h at 4°C. Immunocomplexes were eluted by a c-Myc–tagged peptide solution (MBL, Woburn, MA). The samples after immunoprecipitation were treated with 250 mU of N-glycosidase F (Roche, Mannheim, Germany) for 3 h at 37°C.

Western blotting. The total cellular protein was electrophoretically separated using SDS-12% polyacrylamide gels and transferred onto polyvinylidene difluoride membrane. The membrane was blocked in TBS-Tween containing 5% skim milk for 1 h and then probed with anti-Myc mouse monoclonal antibody (Cell Signaling Technology, Danvers, MA) at 4°C overnight. Horseradish peroxidase–conjugated anti-rabbit antibody and SuperSignal West Pico System (Pierce) were used for the detection of blots.

Real-time RT-PCR. Total RNA was isolated using RNeasy Mini Kit (Qiagen K.K., Tokyo, Japan) and was reverse transcribed using SuperScript III First-Strand Synthesis System (Invitrogen). The mRNA levels were evaluated using ABI PRISM 7900 Sequence Detection System (Applied Biosystems). Ready-to-use assays (Applied Biosystems) were used for the quantification of ADAM10 (Hs00153853_m1), ADAM17 (Hs00234221_m1), MICA (Hs00792195_m1), β-actin (Hs99999903_m1), and CD44 (Hs00174139_m1) mRNAs according to the manufacturer's instructions. The thermal cycling conditions for all genes were 2 min at 50°C and 10 min at 95°C, followed by 40 cycles at 95°C for 15 s and 60°C for 1 min. β-Actin mRNA from each sample was quantified as an endogenous control of internal RNA.

WST-8 assay. HepG2 and PLC/PRF/5 cells were treated with different concentrations of epirubicin for 24 h. Cell growth of epirubicin-treated HCC cells was determined by WST-8 assay (Nacalai Tesque, Kyoto, Japan) as previously described (21).

NK cell analysis. NK cells were isolated from human peripheral blood mononuclear cells by magnetic cell sorting using CD56 MicroBeads (Miltenyl Biotech, Auburn, CA) as previously described (16). The cytolytic ability of NK cells was assessed by 4-h ^{51}Cr-releasing assay with or without MICA/B-blocking antibody (6D4; ref. 7), which binds to the α1 and α2 domains of MICA and MICB. 6D4 was a generous gift from Drs. Veronika Groh and Thomas Spies (Fred Hutchinson Cancer Research Center, Seattle, WA).

Statistics. All values were expressed as the mean and SD. The statistical significance of differences between the groups was determined by applying Student's t test or two-sample t test with Welch correction after each group

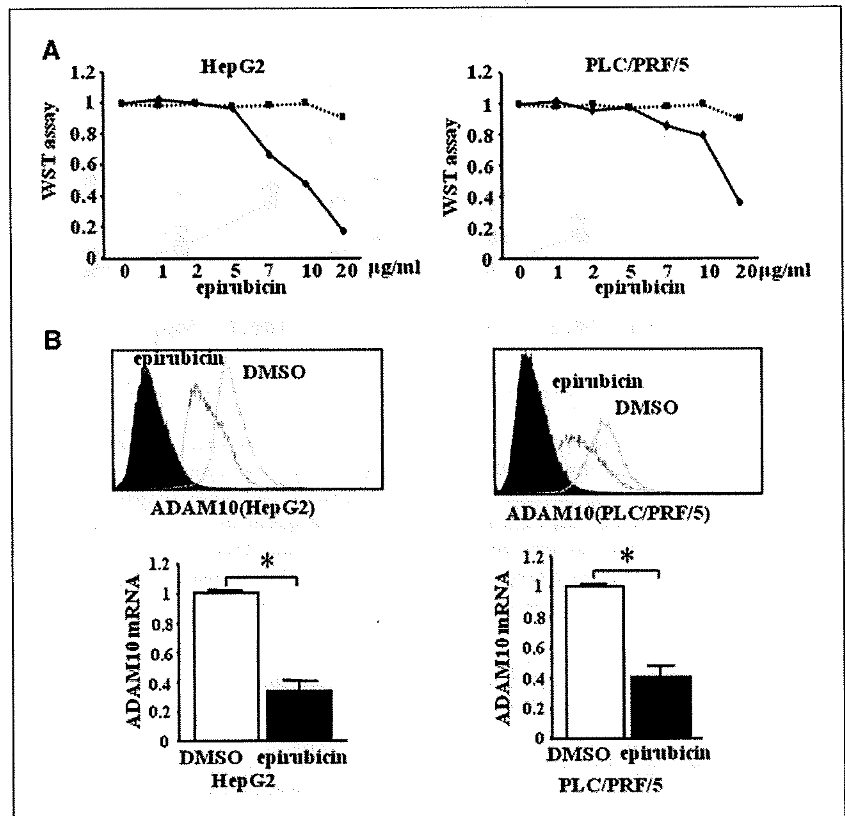

Figure 3. Expression of ADAM10 in epirubicin-treated HCC cells. *A*, the cytotoxicity of epirubicin to human HCC cells was evaluated by WST-8 assay. Cells were treated with different doses of epirubicin (*solid lines*) or vehicle (*DMSO*; *dotted lines*) for 24 h, and the viability of the cells was evaluated by the WST-8 assay. *B*, ADAM10 expression of epirubicin-treated HCC cells. Cells were treated with a nontoxic dose of 1 μg/mL epirubicin (*black lines*) or vehicle (DMSO, *gray lines*) for 24 h and their ADAM10 expression was evaluated by flow cytometry (*top panels*). *Closed histograms*, control IgG staining. Total RNA was extracted at 24 h of epirubicin treatment and mRNA levels of ADAM10 were evaluated by real-time RT-PCR (*bottom panels*). *, $P < 0.05$.

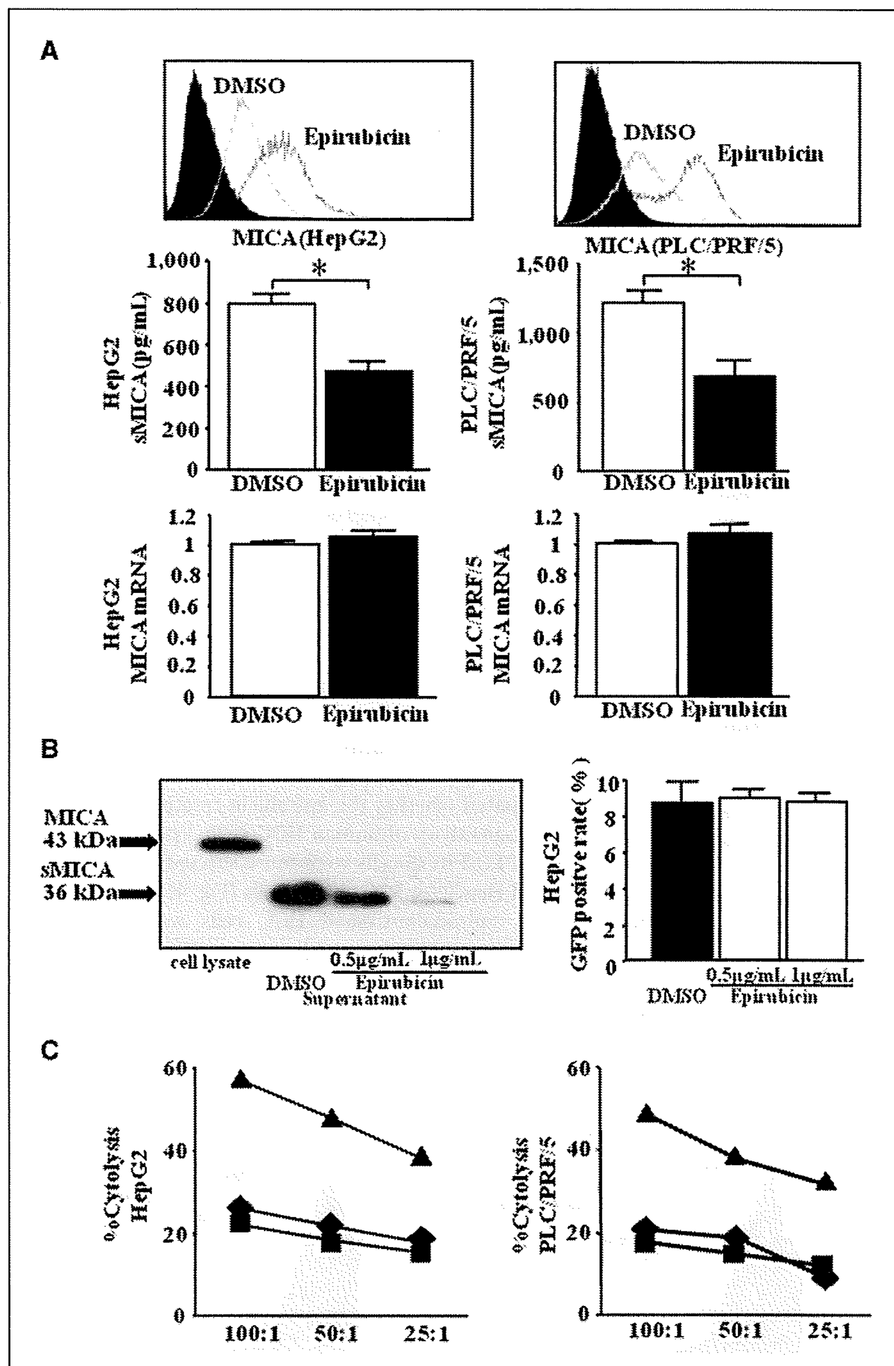

Figure 4. Expression and shedding of MICA in epirubicin-treated HCC cells. *A,* HCC cells were treated with a nontoxic dose of 1 μg/mL epirubicin (*black lines*) or vehicle (DMSO, *gray lines*) for 24 h and their expression of membrane-bound MICA and MICA mRNA was evaluated by flow cytometry (*top panels*) and real-time RT-PCR (*bottom panels*), respectively. *Closed histograms,* control IgG staining in flow cytometry. At the same time, 24-h culture supernatants were subjected to the analysis of soluble MICA (*sMICA*) levels by ELISA (*middle panels*). *, $P < 0.05$. *B,* HepG2 cells were transfected with pMyc-MICA and pEGFP-C1, cultured with 0.5 to 1 μg/mL epirubicin or vehicle (DMSO) for 24 h. Cell lysates from HepG2 cells and 24-h culture supernatants of epirubicin- or vehicle-treated HepG2 cells were immunoprecipitated with anti-Myc. The resulting immunoprecipitates were eluted, treated with N-glycanase, and subjected to Western blot analysis for MICA (*left*). Transfection efficacies were equal in all treatment groups as evidenced by similar GFP-positive cell rates (*right*). *C,* the cytolytic activity of NK cells against HCC cells. Vehicle-treated cells (■) or epirubicin-treated cells without (▲) or with blocking antibody of MICA/B (6D4; ♦) were subjected to ^{51}Cr-release assay. Representative results are shown. Similar results were obtained from three independent experiments.

had been tested with equal variance and Fisher's exact probability test. We defined statistical significance as $P < 0.05$.

Results

ADAM10 and CD44 are overexpressed in human HCC. ADAM10 was detected in all human HCC tissues tested by immunohistochemistry but not in normal liver tissues (Fig. 1*A*). Flow cytometric analysis revealed that ADAM10 was strongly expressed in a variety of HCC cell lines, including HepG2, PLC/PRF/5 (depicted in Fig. 1*B*), and Hep3B (data not shown), but faintly in primary hepatocytes. CD44, a typical substrate of the ADAM10 protease, was also expressed in all human HCC tissues but not in normal liver tissues (Fig. 1*A*). The data suggest that overexpression of ADAM10 and CD44 is a characteristic of human HCC like other malignancies (22).

ADAM10 is involved in MICA shedding of HCC cells but ADAM17 is not. To examine the involvement of ADAM family proteins in MICA ectodomain shedding, ADAM10 or ADAM17 were knocked down in HCC cells using a siRNA-mediated procedure. ADAM10 expression was clearly suppressed in HepG2 cells and PLC/PRF/5 cells at both mRNA and protein levels (Fig. 1*B* and *C*). Both cell lines expressed CD44 on the cellular surface and produced significant levels of soluble CD44 (Fig. 1*D*), indicating that CD44 is expressed and shed from those cell lines. ADAM10 knockdown (KD)

led to an increase in CD44 expression on HCC cells and a decrease in soluble CD44 levels in culture supernatants (Fig. 1*D*). Because ADAM10 has been established as being a sheddase for CD44, siRNA-mediated knockdown of ADAM10 suppressed not only the expression but also the activity of ADAM10 in HCC cells. HepG2 and PLC/PRF/5 cells also expressed ADAM17, which was clearly knocked down by a siRNA-mediated procedure (Fig. 1*B*).

HepG2 cells and PLC/PRF/5 cells expressed membrane-bound MICA and also produced soluble MICA (Fig. 2*A*). Knockdown of ADAM10 for both cell lines clearly upregulated MICA expression on their cellular surface and downregulated soluble MICA levels in their culture supernatant (Fig. 2*A*). In contrast, knockdown of ADAM17 did not affect the expression of membrane-bound MICA or the production of soluble MICA (Fig. 2*B*). We also examined the involvement of ADAM17 in MICA shedding of phorbol 12-myristate 13-acetate (PMA)–stimulated HCC cells because ADAM17 is considered to primarily affect stimulated shedding. The expression of membrane-bound MICA and the soluble MICA production were equal between PMA-stimulated ADAM17KD-HCC cells and control HCC cells (Supplementary Fig. S2). Thus, ADAM10, but not ADAM17, is critically involved in the shedding of MICA in HCC cells.

We next evaluated the cytolytic activity of NK cells against HCC cells. The cytolytic activity of NK cells against ADAM10KD-HepG2 cells was higher than that against control HepG2 cells. This activity was inhibited by blocking of anti-MICA/B antibody, suggesting that the increase of NK sensitivity depended on the increased expression of membrane-bound MICA on ADAM10KD-HepG2 cells, although we could not exclude the possibility of the involvement of MICB in this cytotoxicity (Fig. 2*C*). Similar results were also obtained with ADAM10KD-PLC/PRF/5 cells.

Epirubicin suppresses ADAM10 expression in HCC cells. We examined the biological modification of human HCC cells by adding epirubicin, which is commonly used in anti-HCC chemotherapy. We first examined the cytotoxicity of epirubicin to human HCC cells by WST-8 assay. Adding >5 μg/mL of epirubicin resulted in a significant decrease in cell growth of both HepG2 and PLC/PRF/5 cells (Fig. 3*B*). Based on these findings, we used 1 μg/mL of epirubicin to evaluate the biological effect on human HCC cells without toxicity. Both HepG2 cells and PLC/PRF/5 cells were cultured for 24 h with epirubicin and then subjected to analysis of ADAM10 expression. Epirubicin suppressed ADAM10 expression at the mRNA and protein levels in both cell lines (Fig. 3*C*). Although the data are not shown, doxorubicin also suppressed ADAM10 expression in HCC cells.

Epirubicin inhibits MICA ectodomain shedding and enhances susceptibility to NK cells of HCC cells. The above observations led us to investigate whether epirubicin or doxorubicin treatment would affect MICA ectodomain shedding in HCC cells. Epirubicin treatment led to an increase in membrane-bound MICA expression and a decrease in soluble MICA production in both HepG2 and PLC/PRF/5 cells (Fig. 4*A*). The mRNA levels of MICA did not change after exposure to epirubicin in both HCC cells (Fig. 4*A*). Similar data were obtained with doxorubicin-treated cells (data not shown).

To confirm whether the soluble MICA detected by ELISA was actually reflected in the cleaved form, we transfected Myc-tagged MICA into HepG2 cells and collected culture supernatants as well as cellular lysates. Immunprecipitates from these samples with anti-Myc were subjected to Western blot analysis after treatment with N-glycosidase. MICA in the culture supernatants migrated faster than cellular MICA (Fig. 4*B*), indicating that the MICA detected by ELISA is actually processed and released from full-length MICA. Epirubicin treatment led to a decrease in soluble MICA protein in HepG2 cells (Fig. 4*B*).

We next evaluated whether the epirubicin treatment could also modify the NK sensitivity of human HCC cells. Epirubicin-treated HepG2 cells or PLC/PRF/5 cells were more susceptible to NK cells than nontreated HepG2 or PLC/PRF/5 cells (Fig. 4*C*). The cytolytic activity against epirubicin-treated HCC cells was significantly decreased to the control levels by adding the anti-MICA/B blocking antibody. These results showed that the addition of epirubicin enhanced the NK sensitivity of HCC cell through increased

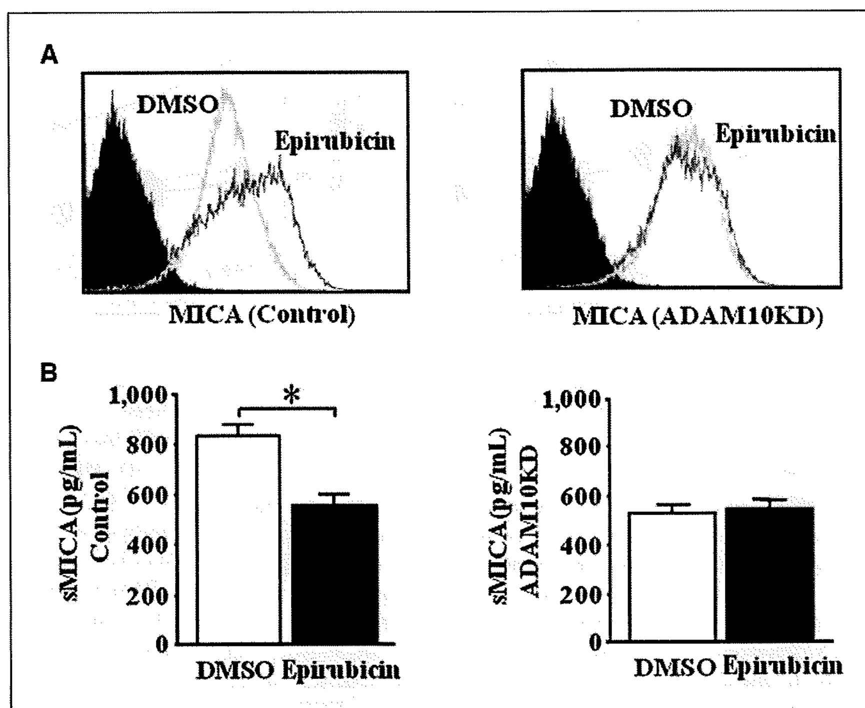

Figure 5. The epirubicin-mediated modification of MICA is ADAM10 dependent. HepG2 cells were transfected with ADAM10 siRNA (*ADAM10KD*) or control siRNA (*Control*) and further cultured with 1 μg/mL of epirubicin (*black lines*) or vehicle (DMSO, *gray line*) for 24 h. The expression of membrane-bound MICA (*MICA*) was evaluated by flow cytometry (*A*), and the soluble MICA (*sMICA*) production in the culture supernatant was evaluated by specific ELISA (*B*). Similar results were obtained from two independent experiments. *, $P < 0.05$.

expression of membrane-bound MICA, although the possibility of MICB involvement could not be excluded. The doxorubicin-treated human HCC cells showed similar results to those obtained from epirubicin-treated HCC cells (data not shown).

Epirubicin inhibits MICA ectodomain shedding through suppression of ADAM10. To examine whether the suppressive effect of epirubicin on MICA shedding occurred through downregulation of ADAM10, HepG2 cells were transfected with ADAM10 siRNA or scramble siRNA as a control and then treated with epirubicin. Consistent with earlier observations, epirubicin upregulated MICA surface expression and downregulated the levels of soluble MICA in control cells (Fig. 5). In contrast, neither upregulation of surface MICA nor downregulation of soluble MICA levels was observed in ADAM10KD-HepG2 cells. These results suggest that the suppressive effect of epirubicin on MICA shedding is mediated by ADAM10 downregulation. We also found similar results with ADAM10KD-PLC/PRF/5 cells (data not shown).

Soluble CD44 and soluble MICA levels in patients with HCC. We have shown that ADAM10 is expressed in human HCC tissues. However, it is not clear whether ADAM10 activity in HCC tissues is actually involved in MICA shedding in patients. Because ADAM10 was reported to be the constitutive functional sheddase of CD44 (23), we examined the soluble CD44 levels in HCC patients, which might be produced from tumor cells through ADAM10 activity. As shown in Fig. 6*A*, the soluble CD44 levels in HCC patients (n = 97) were significantly higher than those in age-matched healthy volunteers (n = 32). More importantly, soluble MICA levels in HCC patients significantly correlated with soluble CD44 levels (Fig. 6*B*), suggesting a close link between MICA shedding and ADAM10 activity.

We further examined soluble CD44 levels before and 2 weeks after TACE in HCC patients. Whereas the levels did not change in nontreated HCC patients during the 2-week interval (n = 9; 306.7 ± 82.5 ng/mL and 309.9 ± 79.9 ng/mL after 2 weeks), they were significantly decreased in epirubicin-based TACE-treated HCC patients (n = 21; 339.7 ± 78.1 ng/mL before TACE and 308.9 ± 81.4 ng/mL after TACE, $P < 0.003$). The changes of soluble CD44 in TACE treatment correlated significantly with those of soluble MICA ($P = 0.0002$; Fig. 6*C*). These results indicated that ADAM10-mediated CD44 shedding was decreased after TACE in HCC patients, implying that this reduction of ADAM10 activity might be related to the decline in MICA shedding.

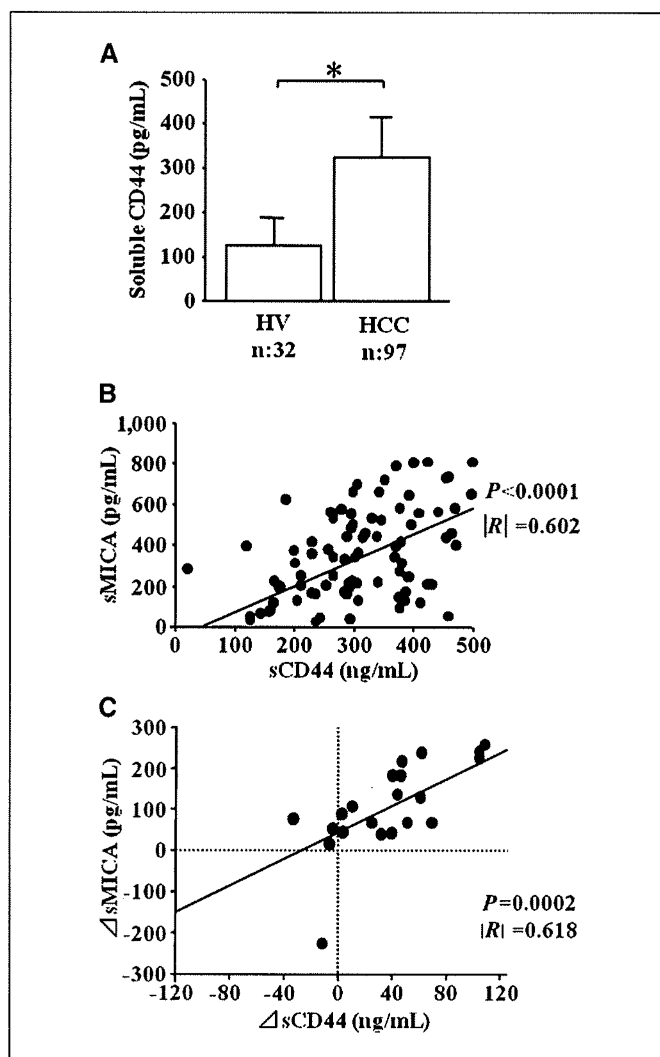

Figure 6. Correlation between soluble CD44 and soluble MICA in human HCC patients. *A* and *B*, soluble CD44 levels and MICA levels in healthy volunteers and HCC patients. Soluble CD44 levels (*sCD44*) and soluble MICA levels (*sMICA*) were determined for sera of HCC patients (n = 97) and age-matched healthy volunteers (*HV*; n = 32). *A*, comparison of sCD44 levels between groups; *B*, correlation between sCD44 levels and sMICA levels in 97 HCC patients. *, $P < 0.05$. *C*, correlation of sCD44 levels and sMICA levels during TACE therapy. HCC patients (n = 21) treated with epirubicin-based TACE therapy were enrolled and examined for sMICA and sCD44 levels before and 2 wk after therapy. Changes in sMICA (ΔsMICA = serum level of sMICA before TACE treatment − serum level of sMICA after TACE treatment) and those in sCD44 levels (ΔsCD44 = serum level of sCD44 before TACE treatment − serum level of sCD44 after TACE treatment) are plotted.

Discussion

MICA shedding is thought to be a principal mechanism by which tumor cells escape from NKG2D-mediated immunosurveillance (13). Thus, inhibition of MICA shedding should be a reasonable strategy for enhancing antitumor immunity. In the present study, we showed that ADAM10 was overexpressed in human HCC tissues and that ADAM10 knockdown resulted in increased expression of membrane-bound MICA, decreased production of soluble MICA, and upregulation of NK sensitivity of human HCC cells. These results point to ADAM10 as a therapeutic target for inhibiting MICA shedding, thereby ameliorating immunity against HCC. Waldhauer and colleagues recently showed that both ADAM10 and ADAM17 proteases are critically involved in the proteolytic release of soluble MICA of human 293T fibroblast cells and HeLa cervix carcinoma cells (20). Interestingly, in the present study, ADAM17 knockdown failed to affect MICA expression in human HepG2 cells or PLC/PRF/5 cells. Thus, ADAM10, not ADAM17, plays an essential role in the shedding of MICA in human HCC cells. Anderegg and colleagues (23) reported that only ADAM10, not ADAM17, contributed to shedding of CD44 molecules in human melanoma cells although both ADAM10 and ADAM17 proteases were significantly expressed in human melanoma tissues, suggesting that ADAM10 and ADAM17 do not always work in a similar manner. A recent report showed that ADAM10, but not ADAM17, could directly bind to calmodulin (24), which may involve the difference of MICA cleavage between ADAM10 and ADAM17 proteases. Recently, Boutet and colleagues reported that ADAM17 regulates proteolytic shedding of the MICB protein, which is another ligand for the NKG2D receptor on immune cells (25). We previously showed that both soluble MICA and MICB significantly increased in the sera of HCC patients and that therapeutic intervention for HCC leads to reduction of soluble

MICA levels, but not of soluble MICB levels (17), suggesting a more important role of soluble MICA in regulating NKG2D expression after HCC therapy. This led us to focus on the mechanism of MICA shedding in the present study.

Our results revealed that anticancer drugs such as epirubicin and doxorubicin downregulated ADAM10 expression and activity, thereby inhibiting MICA ectodomain shedding. The ADAM family proteins, which are highly expressed in some tumors, play a role in secreting growth factors, such as HB-EGF, and migration of cells. Thus, it is speculated that these proteins could be potential targets for tumor treatment (22). The present study is the first to show that clinically available anticancer drugs have an ability to modulate the expression of ADAM family proteins. They seem to suppress ADAM10 expression at a transcriptional level, but the precise mechanism of this suppression is not yet known.

The MICA ELISA system may not equally detect all soluble MICA (MICA molecules have >60 allelic variants). Our finding that soluble MICA could be detected in all HCC patients suggests that this system was applicable for our cohort of HCC patients. However, special caution should be paid for the use of this ELISA system for widely polymorphic MICA. Because CD44 is well known to be released into circulation from tumors by proteolytic cleavage of ADAM10 (23), the activity of ADAM10 in HCC tissues may be correlated with soluble CD44 levels. If so, our data suggest a close link between ADAM10 activity and the shedding of MICA in HCC. Furthermore, the decline in soluble MICA levels correlated well with the decline in soluble CD44 levels as early as 2 weeks after epirubicin-based TACE therapy. Reducing the tumor volume by such therapy may have led to both decreases but it is also possible that epirubicin suppresses ADAM10 activity, thereby inhibiting the shedding of MICA and CD44. Epirubicin may have a previously unrecognized role in cancer therapy; that is, affecting ADAM10 activity and MICA shedding rather than simply serving as a direct toxic agent for tumor cells.

Our data suggest that anti-HCC chemotherapy could remodel HCC cells, enhancing sensitivity to NK cells by upregulating MICA expression on the cellular surface. A concomitant decline in soluble MICA levels ameliorates NK cell ability by upregulating its NKG2D expression. We previously showed that activation of local innate antitumor immunity in liver tissues resulted in eliciting tumor-specific acquired immunity (21). If liver innate immunity is efficiently activated after anti-HCC chemotherapy, an additional antitumor effect against HCC cells could be expected. Immune modulators such as α-galactosylceramide have been shown to efficiently activate liver innate immune cells, including NK cells (21, 26). The combination therapy of anti-HCC chemotherapy and immunotherapy targeting NK cells might improve the antitumor effect of unresectable HCC and the prognosis of HCC patients.

In spite of recent progress in HCC therapies, there remains significant room for improvement, especially with respect to advanced liver cancer. We have shown here that anti-HCC chemotherapy resulted in enhanced NK sensitivity of HCC cells through inhibition of the activity of ADAM10 protease followed by modification of MICA expression. These findings indicate that efficient activation of liver innate immunity after anti-HCC chemotherapy might represent a particularly promising approach to suppress tumor growth and promote regression in liver cancer patients.

Disclosure of Potential Conflicts of Interest

No potential conflicts of interest were disclosed.

Acknowledgments

Received 3/4/09; revised 7/15/09; accepted 7/24/09; published OnlineFirst 10/13/09.

Grant support: Grant-in-Aid from the Ministry of Education, Culture, Sports, Science and Technology of Japan (T. Takehara) and Grant-in-Aid for Research on Hepatitis and BSE from the Ministry of Health, Labour and Welfare of Japan (N. Hayashi).

The costs of publication of this article were defrayed in part by the payment of page charges. This article must therefore be hereby marked *advertisement* in accordance with 18 U.S.C. Section 1734 solely to indicate this fact.

References

1. Fattovich G, Stroffolini T, Zagni I, Donato F. Hepatocellular carcinoma in cirrhosis: incidence and trends. Gastroenterology 2004;127:S35–50.
2. Bosch FX, Ribes J, Diaz M, Cleries R. Primary liver cancer: worldwide incidence and trends. Gastroenterology 2004;127:S5–16.
3. Takayasu K, Arii S, Ikai I, et al. Prospective cohort study of transarterial chemoembolization for unresectable hepatocellular carcinoma in 8510 patients. Gastroenterol 2006;131:461–9.
4. Doherty DG, O'Farrelly C. Innate and adaptive lymphoid cells in human liver. Immunol Rev 2000;174: 5–20.
5. Mehal WZ, Azzaroli F, Crispe IN. Immunology of the healthy liver: old questions and new insights. Gatsroenterology 2001;120:250–60.
6. Bauer S, Groh V, Wu J, et al. Activation of NK cells and T cells by NKG2D, a receptor for stress-inducible MICA. Science 1999;285:727–9.
7. Groh V, Rhinehart R, Seceist H, Bauer S, Grabstein KH, Spies T. Broad tumor-associated expression and recognition by tumor-derived γδT cells of MICA and MICB. Proc Natl Acad Sci U S A 1999;96:6879–84.
8. Jinushi M, Takehara T, Tatsumi T, et al. Expression of MICA and MICB in human hepatocellular carcinomas and their regulation by retinoic acids. Int J Cancer 2003; 104:354–61.
9. Wu JD, Higgins LM, Steinle A, Cosman D, Haugk K, Plymate SR. Prevalent expression of the immunostimulatory MHC class I chain-related molecule is counteracted by shedding in prostate cancer. J Clin Invest 2004; 114:560–8.
10. Raffaghello L, Prigione I, Airoldi I, et al. Downregulation and/or release of NKG2D ligands as an immune evasion strategy of human neuroblastoma. Neoplasia 2004;6:558–68.
11. Ogasawara K, Lanier LL. NKG2D in NK and T cell-mediated immunity. J Clin Immunol 2005;25:534–40.
12. Coudert JD, Held W. The role of the NKG2D receptor for tumor immunity. Semin Cancer Biol 2006; 16:333–43.
13. Groh V, Wu J, Yee C, Spies T. Tumor-derived soluble MIC ligands impair expression of NKG2D and T cell activation. Nature 2002;419:734–8.
14. Salih HR, Rammensee HG, Steinle A. Downregulation of MICA on human tumors by proteolytic shedding. J Immunol 2002;169:4098–102.
15. Salih HR, Antropius H, Gieseke F, et al. Functional expression and release of ligands for activating immunoreceptor NKG2D in leukemia. Blood 2003;102: 1389–96.
16. Jinushi M, Takehara T, Tatsumi T, et al. Impairment of natural killer cell and dendritic cell functions by soluble form of MHC class I-related chain A in advanced human hepatocellular carcinoma. J Hepatol 2005;43: 1013–20.
17. Kohga K, Takehara T, Tatsumi T, et al. Serum levels of soluble major histocompatibility complex (MHC) class I-related chain A in patients with chronic liver disease and changes during transcatheter arterial embolization for hepatocellular carcinoma. Cancer Sci 2008;99:1643–9.
18. Holdenrieder S, Stieber P, Peterfi A, Nagel D, Steinle A, Salih HR. Soluble MICA in malignant disease. Int J Cancer 2006;118:684–7.
19. Kaiser BK, Yim D, Chow IT, et al. Disulphide-isomerase-enabled shedding of tumor-associated NKG2D ligands. Nature 2007;447:482–6.
20. Waldhauer I, Goehlsdorf D, Gieseke F, et al. Tumor-associated MICA is shed by ADAM proteases. Cancer Res 2008;68:6368–76.
21. Tatsumi T, Takehara T, Yamaguchi S, et al. Intrahepatic delivery of α-galactosylceramide-pulsed dendritic cells suppresses liver tumor. Hepatology 2007;45:22–30.
22. Mochizuki S, Okada Y. ADAMs in cancer cell proliferation and progression. Cancer Sci 2007;98:161–7.
23. Anderegg U, Eichenberg T, Parthaune T, et al. Simon JC. ADAM10 is the constitutive functional sheddase of CD44 in human melanoma cells. J Invest Dermatol 2009; 129:1471–82.
24. Nagano O, Murakami D, Hartmann D, et al. Cell-matrix interaction via CD44 is independently regulated by different metalloproteinases activated in response to extracellular domain Ca^{2+} influx and PKC activation. J Cell Biol 2004;165:893–902.
25. Boutet P, Aguera-Gonzalez S, Atkinson S, et al. The metalloproteinase ADAM17/TNF-α enzyme regulates proteolytic shedding of the MHC class I-related chain B protein. J Immunol 2009;182:49–53.
26. Miyagi T, Takehara T, Tatsumi T, et al. CD1d-mediated stimulation of natural killer T cells selectively activates hepatic natural killer cells to eliminate experimentally disseminated hepatoma cells in murine liver. Int J Cancer 2003;106:81–9.

Journal of Viral Hepatitis, 2009, **16**, 844–852 doi:10.1111/j.1365-2893.2009.01131.x

Enhanced ability of regulatory T cells in chronic hepatitis C patients with persistently normal alanine aminotransferase levels than those with active hepatitis

I. Itose,[1] T. Kanto,[1] N. Kakita,[1] S. Takebe,[1] M. Inoue,[1] K. Higashitani,[1] M. Miyazaki,[1] H. Miyatake,[1] M. Sakakibara,[1] N. Hiramatsu,[1] T. Takehara,[1] A. Kasahara[2] and N. Hayashi[1]
[1]*Department of Gastroenterology and Hepatology, Osaka University Graduate School of Medicine, Suita, Japan; and* [2]*Department of General Medicine, Osaka University Hospital, Suita, Japan*

Received December 2008; accepted for publication February 2009

SUMMARY. In hepatitis C virus (HCV) infection, the Th1-type immune response is involved in liver injury. A predominance of immunosuppressive regulatory T cells (Treg) is hypothesized in patients with persistently normal alanine aminotransferase (PNALT). Our aim was to clarify the role of Treg in the pathogenesis of PNALT. Fifteen chronically HCV-infected patients with PNALT, 21 with elevated ALT (CH) and 19 healthy subjects (HS) were enrolled. We determined naturally-occurring Treg (N-Treg) as CD4+CD25high+ FOXP3+ T cells. The expression of FOXP3 and CTLA4 in CD4+CD25high+ cells was quantified by real-time reverse transcriptase-polymerase chain reaction. Bulk or CD25-depleted CD4+ T cells cultured with HCV-NS5 loaded dendritic cells were assayed for their proliferation and cytokine release. We examined CD127–CD25–FOXP3+ cells as distinct subsets other than CD25+ N-Treg. The frequencies of N-Treg in patients were significantly higher than those in HS. The FOXP3 and CTLA4 transcripts were higher in PNALT than those in CH. The depletion of CD25+ cells enhanced HCV-specific T cell responses, showing that co-existing CD25+ cells are suppressive. Such inhibitory capacity was more potent in PNALT. The frequency of CD4+CD127–CD25–FOXP3+ cells was higher in CH than those in PNALT. Treg are more abundant in HCV-infected patients, and their suppressor ability is more potent in patients with PNALT than in those with active hepatitis.

Keywords: HCV, PNALT, regulatory T cell.

INTRODUCTION

Hepatitis C virus (HCV) causes a wide range of chronic liver diseases in infected hosts, including chronic hepatitis (CH), liver cirrhosis and hepatocellular carcinoma (HCC).

Abbreviations: ALT, alanine aminotransferase; CH, chronic hepatitis; CTL, cytotoxic T lymphocyte; DC, dendritic cell; ELISA, enzyme-linked immunosorbent assay; FACS, fluorescence-activated cell sorting; FBS, fetal bovine serum; HBV, hepatitis B virus; HCC, hepatocellular carcinoma; HCV, hepatitis C virus; HS, healthy subjects; IFN, interferon; IL, interleukin; IU, international units; MoDC, monocyte-derived dendritic cell; N-Treg, naturally occurring regulatory T cell; PNALT, persistently normal ALT; RT-PCR, reverse transcriptase-polymerase chain reaction; SLE, systemic lupus erythematosus; TGF, transforming growth factor; Treg, regulatory T cell.

Correspondence: Norio Hayashi, MD, PhD, Department of Gastroenterology and Hepatology, Osaka University Graduate School of Medicine, 2-2 Yamadaoka, Suita, Japan. E-mail: hayashin@gh.med.osaka-u.ac.jp

One of the critical determinants promoting the development of HCV-induced liver disease is sustained liver inflammation, explaining the therapeutic rationale of alleviating this condition to help prevent liver cancer [1]. Among chronically infected individuals, approximately 20–30% display persistently normal serum alanine aminotransferase levels [2,3]. Although it is reported that 40–50% of them progress to the active stage of liver inflammation within 5 years of observation [4], the incidence of HCC in the remaining patients continues to be lower than in those with elevated serum ALT levels [5]. Cumulative studies have revealed that HCV is not directly cytopathic to hepatocytes. It has been demonstrated that a Th1-type or cytotoxic T lymphocyte (CTL) response is critically involved in HCV-mediated liver injury [6,7]. Therefore, it is conceivable that some suppressor mechanisms exist against Th1-type immune responses in patients with persistently normal ALT levels (PNALT), which may be distinct from those in patients with active liver inflammation.

© 2009 The Authors.

Regulatory T cells (Treg) are a unique subset of T cells with inhibitory capacity against auto-reactive T cells [8]. Substantial data have been reported about the involvement of Treg in the pathogenesis of various diseases, including autoimmune, cancer or infectious diseases [9–13]. Currently, the existence of several types of Treg has been reported [14]. Naturally occurring Treg (N-Treg) are derived from the thymic stromal environment from progenitor cells and suppress auto-reactive T cells in antigen-specific and antigen-nonspecific manner. Forkhead/winged helix transcription factor (FOXP3) is one of the specific markers of N-Treg, the expression of which is well correlated with the gain of a suppressor function [15,16]. As cells with high expression of CD25 also display FOXP3, it is generally accepted that CD25+FOXP3+ is the most reliable marker for Treg. In HCV infection, several reports have described a higher frequency of N-Treg in the periphery and the liver [17–20], suggesting their active role in HCV persistence. It has also been demonstrated that CD25+FOXP3+ regulatory cells are inducible in the periphery [21]. Owing to the lack of a specific phenotypic marker of these induced regulatory cells, referred to as adaptive Treg, their role in the pathogenesis of HCV infection has not been clearly understood. A recent study has demonstrated that the expression of interleukin (IL)-7 receptor (CD127) is downregulated in Treg to a degree that is inversely correlated with FOXP3 expression [22]. These findings offer the possibility that adaptive Treg are traceable, not all but in part, by the combination of CD127 and FOXP3 independent of CD25 expression.

In this study, our aim was to elucidate whether or not Treg are involved in the pathogenesis of PNALT patients, by comparing the frequency and function of these cell subsets with those in active hepatitis patients or healthy subjects. A distinct equilibrium was found between N-Treg and CD127–CD25–FOXP3+ T cells according to differences in liver inflammation.

MATERIALS AND METHODS

Subjects

Among chronically HCV-infected patients who had been followed at Osaka University Hospital, 15 patients with PNALT levels and 21 patients with elevated or fluctuating ALT levels (the CH group) were enrolled in this study. As controls, 19 healthy subjects (HS) who were negative for HCV and hepatitis B virus (HBV) markers were examined. The study protocol was approved by the ethical committee of Osaka University Graduate School of Medicine. At enrolment, written informed consent was obtained from each subject. In this study, PNALT patients were defined as those whose ALT levels remained within the normal range (<30 IU/mL) without any medications for more than 1 year. At enrolment, the patients were confirmed to be positive for both serum anti-HCV and HCV RNA, but were negative for other viral infections, including HBV and human immunodeficiency virus. The presence of other causes of liver disease, such as autoimmune, alcoholic and metabolic disorders was excluded by the use of laboratory and imaging analyses. Liver biopsy was carried out in some of the patients. Histological examination was performed according to the METAVIR scoring system. In all patients, a combination of repetitive biochemical tests, ultrasonography or computed tomography scans ruled out the presence of cirrhosis and liver tumours. The clinical background of the subjects are shown in Table 1.

Table 1 Baseline clinical characteristics of the patients

	Chronic hepatitis patients	Patients with PNALT	Healthy subjects*	
n	21	15	19	
Sex (M/F)	8/13	5/10	ND	NS
Age	50.6 ± 11.6	47.8 ± 12.7	ND	NS
ALT (IU/L)	88.3 ± 41.4	20.9 ± 6.9	ND	$P < 0.0001^{\dagger}$
Plt ($10^4/\mu L$)	13.5 ± 5.4	20.0 ± 3.9	ND	$P < 0.01^{\dagger}$
HCV RNA (Meq/mL)	8.6 ± 11.3	9.7 ± 7.8	ND	NS

*The background data of healthy subjects (blood donors) were not accessible owing to the confidentiality regulations of the blood centre, but their serum ALT levels were confirmed to be within the normal range. †Statistical significance was analysed by Mann–Whitney U test between chronic hepatitis patients and patients with PNALT. The values are expressed as mean ± SD. PNALT, persistently normal alanine aminotransferase level; ND, not determined; NS, not significant; plt, platelet count.

© 2009 The Authors.

Frequency analyses of Treg cells

For the numerical analyses of Treg cells, heparinized venous blood was obtained from all subjects. Peripheral blood mononuclear cells were collected by density-gradient centrifugation on a Ficoll–Hypaque cushion. The cells were subsequently stained with a combination of various fluorescence-labelled anti-human mouse monoclonal antibodies for phenotypic markers. The antibodies for CD25 (clone B1.49.9) and CD4 (clone 13B8.2) were purchased from Beckman Coulter (Fullerton, CA, USA), that for CD127 (clone 40131) from R&D Systems (Minneapolis, MN, USA) and that for FOXP3-PE (clone PCH101) from eBioscience (San Diego, CA, USA), respectively. The cells were stained in phosphate-buffered saline containing 1% fetal bovine serum (FBS) with various antibodies or isotype controls for 15 min at room temperature. Intracellular staining of FOXP3 was performed using a human FOXP3 staining kit (eBioscience) according to the manufacturer's instructions. The cells were analysed by FACSCalibur (BD Biosciences, San Jose, CA, USA) and CellQuest software.

Functional analysis of CD4+CD25+ T cells in HCV-specific CD4+ T cell response

We first examined the HCV-specific CD4+ T cell response in the presence or absence of CD4+CD25+ T cells. Monocyte-derived dendritic cells (MoDC) were generated from CD14+ cells as reported previously. In brief, CD14+ cells were cultured in Iscove's modified Dulbecco's medium (Gibco Laboratories, Grand Island, NY, USA) supplemented with 10% FBS, 50 IU/mL of penicillin, 50 mg/mL of streptomycin, 2 mM of L-glutamine, 10 mM of Hepes buffer, 10 mM of nonessential amino acids in the presence of 50 ng/mL of granulocyte/macrophage colony-stimulating factor (PeproTech, Rocky Hill, NJ, USA) and 10 ng/mL of IL-4 (PeproTech) for 7 days at 37 °C and 5% CO_2. On day 6 of the culture, MoDC were pulsed with 10 μg/mL of recombinant HCV NS5 (amino acid position: NS5B 1-544; kindly provided by Japan Tobacco, Inc., Tokyo, Japan) and cultured for 24 h. The antigen-pulsed MoDC were then cultured with autologous bulk CD4+ T cells or CD4+CD25– T cells in 96-well flat-bottom plates (Corning, NY, USA) for 5 days. Enrichment of CD4+ T cells or CD4+CD25– T cells was performed using a CD4+CD25+ Regulatory T cell Isolation kit (Miltenyi Biotec, Auburn, CA, USA) according to the manufacturer's instructions. On day 6 of the co-culture, the cells were pulsed with 1 μCi of [3H]-thymidine during the last 16 h of incubation. The supernatants were collected before pulsing with [3H]-thymidine and subjected to cytokine enzyme-linked immunosorbent assay (ELISA). The incorporation of [3H]-thymidine in CD4+ T cells was measured using a β-counter (Wallac-Perkin-Elmer, Wallac, Finland).

Enzyme-linked immunosorbent assay

The concentrations of IL-10, TGF-β1 and interferon (IFN)-γ in the culture supernatants were determined by ELISA. We used matched pairs of relevant monoclonal antibodies (Endogen, Woburn, MA, USA) for IL-10 and IFN-γ, and the DuoSet ELISA development system (R&D Systems) for TGF-β1, according to the manufacturer's instructions. The detection thresholds of IL-10, TGF-β1 and IFN-γ were 10, 10 and 16 pg/mL, respectively.

Real time reverse transcriptase-polymerase chain reaction (RT-PCR)

In order to analyse the expression of FOXP3 and CTLA-4 in N-Treg, we collected CD4+CD25high T cells by using FACSAria. The purity of the isolated cells was more than 95% as determined by FACS. Total RNA was extracted from sorted CD4+CD25high T cells using the RNeasy Mini Kit (Qiagen, Valencia, CA, USA) according to the manufacturer's instructions. Complementary DNA was synthesized using the SuperScript III First-Strand synthesis system (Invitrogen, Carlsbad, CA, USA). Assays-on-demand primers and probes (PE Applied Biosystems, Foster City, CA, USA) were used to quantify FOXP3 and CTLA4 expression. The mRNA levels were evaluated using ABI PRISM 7900 Sequence Detection System (Applied Biosystems). The thermal cycling conditions for all genes were as follows: the reaction was started with a 10-min denaturing cycle at 95 °C, followed by 40 cycles of PCR performed with 15 s of denaturing at 95 °C, then 1 minute at 60 °C for annealing and extension. We identified a calibrator sample from the healthy volunteers. The expressions of molecules were given as the relative values to the calibrator samples. To standardize the amount of total RNA added to each reaction mixture, we quantified β-actin mRNA from each sample as a control of internal RNA and corrected all values with this.

Statistical analysis

Statistical analyses were performed using StatView 5.0 software (SAS Institute Inc., Cary, NC, USA). Mann–Whitney *U*-test was used to compare differences in unpaired samples. For all analyses, a *P*-value of less than 0.05 was considered to be statistically significant.

RESULTS

Peripheral N-Treg are increased in HCV-infected patients

We compared the frequency of Treg between HCV-infected patients and healthy donors. In HCV-positive individuals, they were further categorized into PNALT and CH groups according to the difference in their serum ALT levels. The clinical backgrounds of these groups were not different except for

© 2009 The Authors.

serum ALT levels and platelet counts (Table 1). N-Treg were defined as the cells with CD4+CD25high+FOXP3+ cells. As the cut-off value between CD25high+ and CD25intermediate+ cells is a critical determinant for Treg analyses, we defined CD4+CD25high+ as the cells with CD25 levels higher than those of CD4–CD25+ cells (Fig. 1a). We first compared the frequency of CD4+FOXP3+ T cells. The frequency of FOXP3+ cells in the CD4+ T cell population in HCV-infected patients was significantly higher than those in the HS (Fig. 1b). However, no difference was observed in FOXP3+ cells between the PNALT and CH patients (Fig. 1b). The frequency of CD4+CD25high+FOXP3+ T cells in CH or PNALT patients were significantly higher than those in HS, whereas those in HCV-positive patients did not differ regardless of their ALT levels (Fig. 1c). Similar results were obtained for the frequency of CD4+CD25–FOXP3+ T cells (Fig. 1d).

Next, we examined whether or not the frequency of N-Treg is correlated with clinical parameters. Among all HCV-infected patients, no correlation was observed between the frequency of N-Treg (CD4+CD25high+ FOXP3+ T cells) and serum ALT, HCV RNA levels, age or platelet counts (data not shown). In the analyses of patients who had undergone liver biopsy, the frequency of N-Treg was not correlated with METAVIR grade/stage scores (data not shown).

The expressions of FOXP3 and CTLA4 are higher in N-Treg from PNALT patients compared with those from the CH group

FOXP3 is the master gene of Treg in the development and gaining of suppressor functions. Alternatively, CTLA4 is one of the key molecules of Treg in exerting inhibitory function. We thus evaluated FOXP3 and CTLA4 mRNA expression in sorted N-Treg (CD4+CD25high+ T cells) by means of real-time RT-PCR. The expression of FOXP3 in PNALT or CH patients was significantly higher than those in HS (Fig. 2a). Of note is the higher expression of FOXP3 in N-Treg from the PNALT group than in those from the CH group (Fig. 2a). In contrast, the expression of CTLA4 in N-Treg from the PNALT was higher than those in the CH, while it did not differ between the CH and HS groups (Fig. 2b).

CD4+CD25+ T cells from PNALT patients have more suppressive capacity in the HCV-specific CD4+ T cell response than those from CH patients

In order to compare the ability of N-Treg to inhibit the antigen-specific CD4+ T cell response, we used autologous MoDC pulsed with HCV proteins as antigen-presenting cells. We examined CD4+ T cell proliferation or cytokine

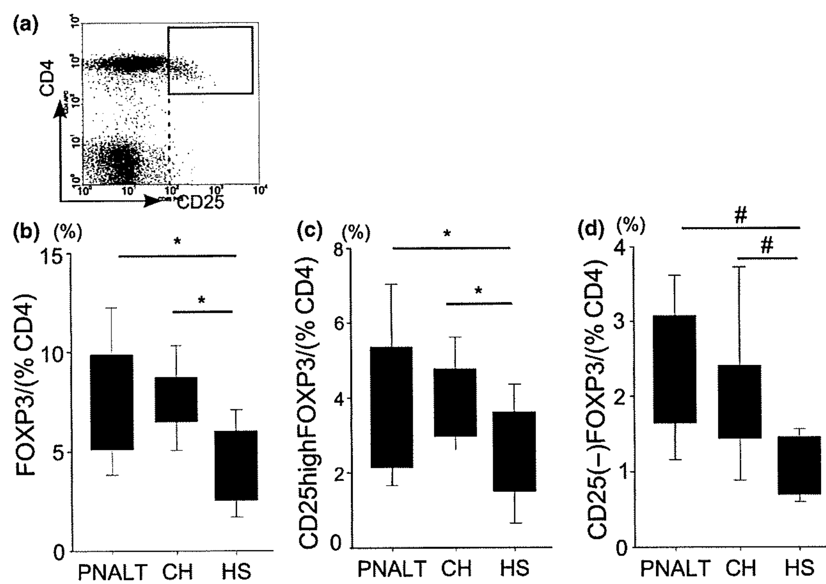

Fig. 1 Comparison of frequencies of naturally-occurring regulatory T cells (N-Treg) and FOXP3-positive cells among the groups. (a) Gating of CD4+CD25high+ T cells under FACS analysis. The cut-off value of CD25high expression is set at a level that is more than that of CD4–CD25+ cells (dotted line); CD4+CD25high+ T cells are shown in the rectangle drawn in the representative dot plot. (b) Frequencies of FOXP3+ cells, (c) N-Treg (CD25high+FOXP3+ cells) and (d) CD25–FOXP3+ cells in CD4+ T cells were compared among the groups. Boxes represent lower and upper quartiles with the median value (solid line) between boxes, while the whiskers represent the minimum and maximum values. *, $P < 0.05$; , $P < 0.0001$ by Mann–Whitney *U*-test. *Abbreviations:* PNALT, hepatitis C virus (HCV)-infected patients with persistently normal alanine aminotransferase (ALT) levels; CH, HCV-infected patients with elevated ALT levels; HS, healthy subjects.

© 2009 The Authors.

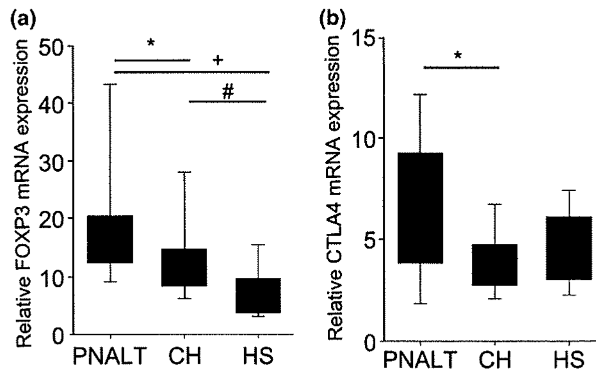

Fig. 2 Comparison of mRNA expression of FOXP3 and CTLA4 in CD4+CD25high+ T cells among the groups. The expression of FOXP3 (a) and CTLA4 (b) in separated CD4+CD25high+ T cells were analysed by real-time reverse transcriptase-polymerase chain reaction as described in Materials and methods. Boxes represent lower and upper quartiles with the median value (solid line) between boxes, while the whiskers represent the minimum and maximum values. *, $P < 0.05$; , $P < 0.01$; +, $P < 0.001$. For definitions of PNALT, CH and HS, see Fig. 1.

production stimulated with antigen-pulsed DC. We compared such responses between samples with or without CD4+CD25+ T cells. In PNALT patients, HCV NS5-specific T cell proliferation or IFN-γ production of CD25-depleted CD4+ T cells was significantly higher than those of the bulk CD4+ T cells (Fig. 3a,b). In contrast, in CH patients, such restoration did not occur significantly even when CD4+ CD25+ T cells had been depleted (Fig. 3a,b). There was no difference in the production of IL-10 and TGF-β between bulk CD4+ T cells and CD25-depleted CD4+ T cells in both CH and PNALT patients (Fig. 3c,d). These results suggest that co-existing CD4+CD25+ T cells play an inhibitory role in the HCV-specific CD4+ T cell response, in which suppression was more potent in the PNALT than in the CH group.

CD127–FOXP3+ cells, regardless of their CD25 expression, are increased in patients with HCV infection

In the analyses of N-Treg, the frequency of CD4+CD25–FOXP3+ T cells in HCV-infected patients was higher than those in the healthy donors (Fig. 1d). These results suggest that CD4+FOXP3+ T cells, regardless of the degree of CD25

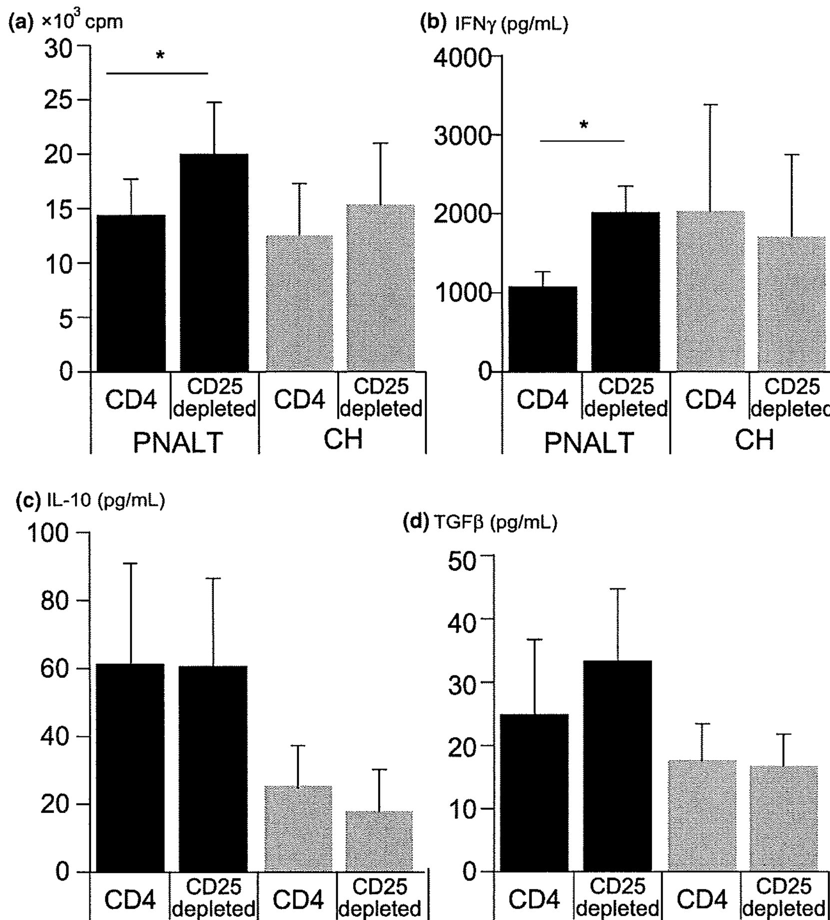

Fig. 3 Changes of hepatitis C virus (HCV)-specific CD4+ T cell responses with or without depletion of CD25+ T cells. Bulk CD4+ T cells or those depleted of CD25+ cells were cultured with autologous monocyte-derived dendritic cells in the presence of HCV-NS5 protein for 5 days as described in Materials and methods. (a) On day 4, [3H]-thymidine was pulsed and the thymidine incorporation was counted with a β-counter. Before the pulsing, the culture supernatants were harvested and subjected to enzyme-linked immunosorbent assay for interferon-γ (b), interleukin-10 (c) and TGF-β (d), respectively. *, $P < 0.05$ by Mann–Whitney *U*-test. For definitions of PNALT and CH, see Fig. 1.

© 2009 The Authors.

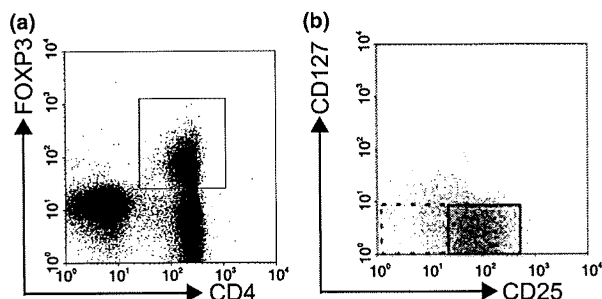

Fig. 4 Gating of CD4+CD127–FOXP3+ cells with variable CD25 expression under FACS analysis. After setting the gate on CD4+FOXP3+ cells [rectangle in the dot plot (a)], were displayed on the CD25 and CD127 axis (b). The presence of CD25+ (bold rectangle) and of CD25– cells (dotted rectangle) in CD4+FOXP3+ cells are shown in plot (b). The frequencies of these cells were analysed.

expression, increase in chronic HCV infection. Alternatively, it implies that higher expression of CD25 is not a universal marker for identifying FOXP3+ cells with regulatory activity. It has been reported that CD127 expression on CD4+ T cells is inversely correlated with FOXP3 expression, suggesting that CD127low/negative cells consist of those with regulatory activity. In order to analyse regulatory T cell subsets more precisely, we first examined FOXP3 expression on CD127– or CD127+ cells paired with CD25 expression in patients with HCV infection (Fig. 4). As a result, the majority of CD4+FOXP3+ T cells belonged to the CD127– population irrespective of CD25 expression (Fig. 4). Next, we compared the frequency of CD4+CD127–FOXP3+ cells, which consist of CD25+ and CD25– cells, among the subject groups (Fig. 5a). The frequency of CD4+CD127–FOXP3+ cells was similar in the CH and the PNALT groups, both of which were significantly higher than those in the HS (Fig. 5a). Finally, in order to estimate the profile of CD4+CD127–FOXP3+ cells according to CD25 expression, we compared the percentage of CD25+CD127–FOXP3+ or CD25–CD127–FOXP3+ cells in CD4+ T cells among the groups. The percentage of CD25+CD127–FOXP3+ T cells in CD4+ T cells was comparable for PNALT and CH (Fig. 5b). In clear contrast, the percentage of CD25–CD127–FOXP3+ T cells in the PNALT was lower than those in the CH (Fig. 5c). The frequencies of these cells were higher in the HCV-infected patients than in HS (Fig. 5b,c). When we set the focus on the proportion of CD25+CD127– or CD25-CD127– cells in the FOXP3+ cells in the periphery as a whole, we found that the proportion of CD25+CD127– cells in the PNALT was higher than that in the CH group (Fig. 5d). On the other hand, the proportion of CD25–CD127– cells in FOXP3+ cells was lower in the PNALT than in the CH group (Fig. 5e). Therefore, the phenotypic profiles of FOXP3+ T cells are distinct between PNALT and CH patients, with regard to the expression of CD127 and CD25.

DISCUSSION

Approximately 30–40% of chronically HCV-infected patients continue to display PNALT for decades. We previously reported the possible contribution of certain human leukocyte antigen haplotypes [23] or DC dysfunction in the maintenance of the PNALT state [24]. However, the precise mechanisms behind this important issue are yet to be

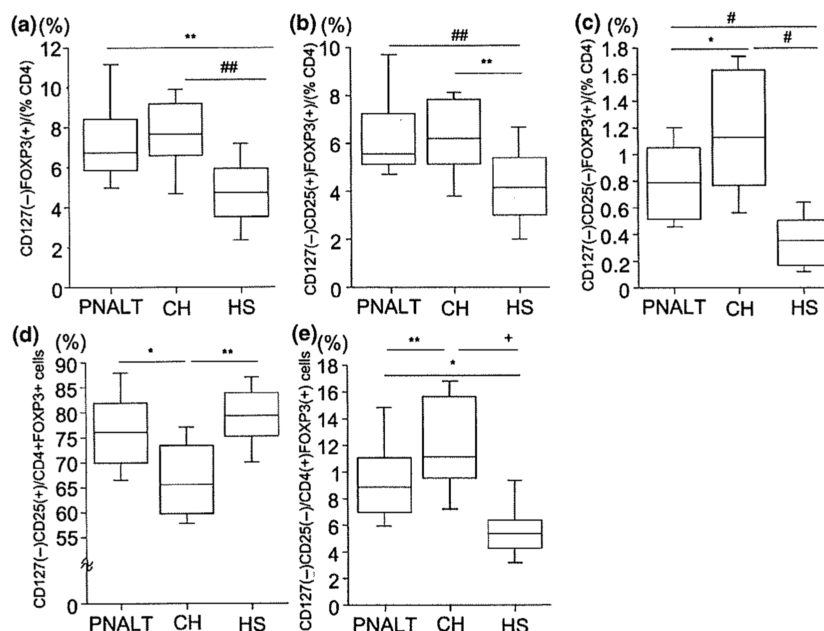

Fig. 5 Comparison in the frequencies of CD127– regulatory T cell subsets among the groups. Frequencies of CD127–FOXP3+ (a), CD127–CD25+FOXP3 (b) and CD127–CD25–FOXP3+ (c) cells among CD4+ T cells were determined by FACS analysis. The proportion of CD127–CD25+ (d) or CD127–CD25– (e) cells in CD4+FOXP3+ cells were also determined. Boxes represent lower and upper quartiles with the median value (solid line) between boxes, while the whiskers represent the minimum and maximum values. *, $P < 0.05$; , $P < 0.01$; **, $P < 0.005$; ##, $P < 0.001$; +, $P < 0.0001$ by Mann–Whitney *U*-test. For definitions of PNALT, CH and HS, see Fig. 1.

© 2009 The Authors.

established. Cumulative reports have shown that Th1/Tc1 type responses are instrumental in HCV-induced liver inflammation [7,25,26]. We thus hypothesized that some suppressor mechanisms exist in PNALT patients especially against HCV-specific Th1 and/or CTL reactions.

The involvement of Treg cells in the pathogenesis of various diseases has been reported [9–13]. Most of the studies presented the possibility that N-Treg play substantial roles in the induction of tolerance against aetiological self or nonself antigens, thus leading to alleviation or exacerbation of the disease severity. With regard to HCV infection, several groups have shown that N-Treg are increased both in the periphery and in the liver and are able to inhibit HCV-specific CD4+ or CD8+ T cell responses *in vitro* [17,18,27]. In this study, we showed that the frequency of N-Treg in HCV-infected patients is higher than those in the controls, which is consistent with the previous reports. However, the frequencies of N-Treg are indistinguishable between the patient groups with different disease activities. As for the functional aspect, the deprivation of CD4+CD25+ cells enhanced the HCV NS5-specific CD4+ T cell response in the PNALT than in the CH group, suggesting that co-existing Treg in the PNALT are more suppressive. In addition, the expression of FOXP3 and CTLA4, which are key molecules of the suppressor function, is higher in PNALT than in those with active hepatitis. Venken *et al.* [28] demonstrated that the degree of FOXP3 expression at the single-cell level of N-Treg is well correlated with their suppressive ability, which is supportive of our results. In contrast, Bolacchi *et al.* [29] reported that the frequency of TGF-β+ N-Treg in the PNALT was higher than in the hepatitis group. Furthermore, their frequency was inversely correlated with the histological inflammatory grade, suggesting that TGF-β+ Treg play active roles in alleviating hepatitis. The reasons for the lack of correlation between N-Treg and serum ALT or HCV RNA quantity in the present study may be because of the difference in the target of analyses, such as either peripheral or intra-hepatic Treg, or either TGF-β+ or bulk Treg. Further analyses need to be performed on these important issues, as CD4+FOXP3+ Treg are reported to accumulate more in the portal tract of HCV-infected livers compared with those in the periphery [20].

During the observation period, about 30–40% of PNALT patients began to show elevated or fluctuating ALT abnormalities. What crucial factor triggers HCV-induced liver inflammation remains unknown. One of the plausible explanations is an antigenic shift accompanied by the occurrence of mutations in the HCV genome. In other words, hepatitis may flare up if the mutation raises HCV immunogenicity. Comprehensive analyses of HCV epitopes for CTL using overlapping peptides have shown that the HCV core and NS3 are more immunogenic than the remaining regions; however, the presence of an epitope hierarchy in Treg induction has been controversial. Li *et al.* [30] reported the possibility that Treg are expandable in response to certain epitopes in HCV proteins. In two patients in whom we observed flare-up of hepatitis in this study, we were able to find that the expression of FOXP3 in N-Treg was high in the PNALT status, but declined in the active hepatitis stage (data not shown). Although it is difficult to state whether such phenotypic changes in N-Treg are the cause or the consequence of disease progression, these results suggest the involvement of N-Treg in the degree of HCV-mediated hepatitis. Further detailed study is needed to examine whether or not such changes in N-Treg are related to the sequence evolution in HCV genomes.

Recent research has disclosed that distinct types of Treg are present in humans. Currently, it is generally accepted that CD25+FOXP3+ is the most reliable marker for Treg, which is induced in parallel with the acquisition of suppressor ability. However, owing to the lack of phenotypic markers for specifically identifying adaptive Treg, their roles in clinical settings have been unclear. In this study, CD4+FOXP3+ cells increased in HCV-infected patients, who were either positive or negative for CD25. In contrast to thymus-derived N-Treg expressing a greater degree of CD25, adaptive Treg are presumed to be induced in the periphery with a lesser degree of CD25 expression. Thus, it is likely that CD4+CD25–FOXP3+ T cells in HCV infection contain some part of adaptive Treg.

Treg have been reported to express low levels of CD127 at their cell surface [31]. Furthermore, the expression of CD127 is inversely correlated with FOXP3 expression and with the suppressive function of CD25high+ Treg. Liu *et al.* [22] pointed out the possibility that adaptive Treg are grouped into CD127– cells, which also include FOXP3-negative Tr1 or Th3 cells. Alternatively, You *et al.* [32] reported that murine CD4+CD25lowFOXP3+ T cells might be adaptive Treg, which exert a TGFβ-dependent suppressive function. Taking these reports into consideration, and in order to exclude activated CD25+ T cells, we examined CD4+ CD127–CD25–FOXP3+ cells tentatively determined as part of adaptive Treg. In order to confirm that CD4+CD127– cells possess suppressive capacity, we co-cultured sorted CD4+CD127–CD25– or CD4+CD127–CD25+ cells with allogeneic CD4+ T cells stimulated with anti-CD3 and anti-CD28 antibodies. As a result, we found that CD4+CD127– cells, regardless of CD25 expression, significantly suppressed the proliferation of responder CD4+ T cells (manuscript in preparation). Of note is the finding that the frequency of CD127–CD25–FOXP3+ cells is higher in patients with active hepatitis than those in the PNALT group. One of the plausible explanations for such an increase of Treg is the compensatory mechanisms for the aggravation of liver inflammation. In support of this possibility, Bonelli *et al.* [33] reported that CD4+CD127–CD25– cells are increased in patients with systemic lupus erythematosus (SLE), the numbers of which are well correlated with disease activity. With regard to the ability of Treg in SLE patients, CD4+CD127–CD25– cells were potent in the inhibition of T

© 2009 The Authors.